

NASA CONTRACTOR
REPORT

NASA CR-1641



NASA CR 16
C.1

0060749



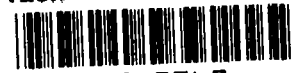
LOAN COPY: RETURN TO
AFWL (DOGL)
KIRTLAND AFB, N. M.

PRECIPITATION STRENGTHENED TANTALUM
BASE ALLOY, ASTAR-811C

by R. W. Buckman, Jr., and R. C. Goodspeed

Prepared by
WESTINGHOUSE ASTRONUCLEAR LABORATORY
Pittsburgh, Pa. 15236
for Lewis Research Center





0060749

1. Report No. NASA CR-1641	2. Government Accession No.	3. Recipient's Catalog No.	
4. Title and Subtitle PRECIPITATION STRENGTHENED TANTALUM BASE ALLOY, ASTAR-811C		5. Report Date March 1971	6. Performing Organization Code
		8. Performing Organization Report No. WANL-PR-(Q)-016	
7. Author(s) R. W. Buckman, Jr., and R. C. Goodspeed		10. Work Unit No.	
9. Performing Organization Name and Address Westinghouse Astronuclear Laboratory Pittsburgh, Pennsylvania 15236		11. Contract or Grant No. NAS 3-2542	
		13. Type of Report and Period Covered Contractor Report	
12. Sponsoring Agency Name and Address National Aeronautics and Space Administration Washington, D. C. 20546		14. Sponsoring Agency Code	
		15. Supplementary Notes	
16. Abstract A creep resistant fabricable tantalum base alloy, Ta-8W-1Re-0.7Hf-0.025C (ASTAR 811C), was developed for potential use as structural and liquid alkali metal containment material in advanced Rankine cycle space nuclear power systems. Preceding the discovery of the ASTAR-811C composition was a detailed study of the Ta-W-Hf-C alloy system with additions of Re, Mo, Zr, and N. Alloy compositions were selected with primary emphasis on improving high temperature creep properties and still maintaining good fabricating and weldability characteristics. All evaluations were performed on 0.04 inch sheet processed from ingot prepared by nonconsumable and consumable electrode arc melting. ASTAR-811C sheet material recrystallized one hour at 3000° F (1650° C) has 25% tensile elongation at -320° F. Recrystallized base metal and electron beam welded material exhibited 1t bend ductility at -320° F, while tungsten-inert-gas (GTA) welded sheet is bend ductile at -175° to -250° F. ASTAR-811C and T-111 (Ta-8W-2Hf) exhibit similar fabricability and ductility characteristics, although the creep strength of ASTAR-811C is approximately double that of T-111 at 2400° F (1315° C).			
17. Key Words (Suggested by Author(s)) Refractory metal alloys Tantalum alloys ASTAR 811-C Mechanical properties Welding Alloy development		18. Distribution Statement Unclassified - unlimited	
19. Security Classif. (of this report) Unclassified	20. Security Classif. (of this page) Unclassified	21. No. of Pages 89	22. Price* \$ 3.00



FOREWORD

The work described in this report was performed by the Westinghouse Astronuclear Laboratory under NASA contract NAS 3-2542 with Mr. Paul E. Moorhead of the Lewis Research Center Space Power Systems Division as the NASA Project Manager. The report was originally issued as Westinghouse report WANL-PR-(Q)-016.



TABLE OF CONTENTS

	<u>Page No.</u>
I. INTRODUCTION	1
II. ASTAR-811C	2
A. CONSOLIDATION	2
B. MICROSTRUCTURE	5
C. RECRYSTALLIZATION BEHAVIOR	5
D. WELDABILITY	10
E. THERMAL STABILITY AND EFFECT OF OXYGEN CONTAMINATION	14
III. ALLOYING EFFECTS IN TANTALUM	35
A. EXPERIMENTAL PROGRAM DESIGN	35
B. EXPERIMENTAL PROCEDURES	36
C. EXPERIMENTAL RESULTS AND DISCUSSION	40
V. CONCLUSIONS	78
REFERENCES	80

LIST OF FIGURES

	Page No.
1. As-Melted Ingot and As-Forged ASTAR-811C	3
2. As-Rolled 1/4" Thick Plate and 0.04" Thick Sheet of ASTAR-811C	4
3. Microstructure and Hardness of ASTAR-811C	7
4. Recrystallization Behavior of ASTAR-811C	9
5. Recrystallization Behavior of ASTAR-811C	11
6. Isothermal Annealing Curves for ASTAR-811C Sheet	12
7. Hardness Traverse and Microstructure of TIG Welded 0.04" Thick ASTAR-811C	16
8. Hardness Traverse for ASTAR-811C Weld Specimens	18
9. Microstructure of ASTAR-811C Welded Specimens	19
10. Tensile Properties of ASTAR-811C	20
11. Tensile Properties of GTA Welded ASTAR-811C Compared with that of 0.04 Inch Sheet	23
12. Creep Properties of ASTAR-811C Compared to T-111 on Parametric Plot of Time to Elongate 1%	24
13. Effect of Final Annealing Temperature on the Shape of the Creep Curve for ASTAR-811C Tested at 2400°F and 15,000 psi	26
14. Electron Micrographs Showing Effect of Final Annealing Temperature on the Carbide Morphology	27
15. Effect of Grain Size and Final Annealing Temperature on Creep Properties of ASTAR-811C	28
16. Effect of Final Annealing Temperature on the R.T. Tensile Properties of ASTAR-811C	30
17. Electron Transmission Photomicrograph of ASTAR-811C Sheet, Annealed 1 Hour at 3630°F and Rapidly Cooled	31
18. Transmission Electron Micrograph of ASTAR-811C Sheet, Annealed 1 Hour at 3630°F, Rapidly Cooled, then Creep Tested at 2400°F and 15,000 psi at 1×10^{-8} Torr.	32
19. Effect of Carbon on the Forgeability Limit, 50% Upset, of Ta-W-Hf Alloys	42

LIST OF FIGURES (CONTINUED)

		<u>Page No.</u>
20.	As-Forged Button and As-Cast Microstructure	43
21.	Effect of Carbon and Nitrogen on the Room Temperature Hardness of As-Cast Tantalum Alloys	44
22.	As Dynapak Extruded Tantalum Alloy Sheet Bar	46
23.	Effect of W, Hf and C on the Secondary Working Characteristics of Tantalum	47
24.	Effect of Carbon on the Bend Ductility of Experimental Tantalum Alloys	49
25.	Effect of Post Weld Annealing on the Fusion Zone Microstructure and Bend DBTT	51
26.	Effect of Carbon and Nitrogen on the Bend Ductile-Brittle Transition Temperature of Experimental Tantalum Alloys	52
27.	Recrystallization Behavior of Experimental Tantalum Alloy Sheet Given a Prior Cold Reduction of 70-75%	54
28.	Aging Response of Nitrogen and Carbon Bearing Tantalum Alloys Solution Annealed for 1 Hour at 2000°C and Rapidly Cooled	55
29.	Microstructure of Ta-5.3W-0.65Mo-1.56Re-0.52Zr-0.08N After Solution Annealing 1 Hour at 3630°F, Rapidly Cooling, and Aging for 1 Hour at the Indicated Temperature	56
30.	Effect of Carbon on the Room Temperature Tensile Properties of Ta(8-9)W-(1-3)Hf Alloys	59
31.	Effect of Carbon on the Elevated Temperature Tensile Strength of Ta-(8-9)W-(1-3)Hf Alloys	63
32.	Typical Creep Curve Shape at 2400°F Obtained in Deadweight Loaded Ultra-High Vacuum Creep System	64
33.	Effect of Carbon on the Creep Behavior of Ta-W-Hf Alloys at 2400°F and 15,000 psi	66
34.	2400°F Creep Behavior of Ta-W-Hf-C Alloys	67
35.	Effect of Reactive Metal (Hf+Zr) Addition on the Creep Behavior of Tantalum Alloys Tested at 2400°F and 15,000 psi	69
36.	Effect of Composition on the Creep Behavior of Experimental Tantalum Alloys	70

LIST OF FIGURES (CONTINUED)

	<u>Page No.</u>
37. Effect of Composition on the Creep Behavior of Experimental Tantalum Alloys	71
38. Effect of Rhenium on the Creep Behavior of Tantalum Alloys	73
39. Creep Behavior of Experimental Tantalum Base Alloys	75

LIST OF TABLES

	<u>Page No.</u>
1. Chemical Analysis Results for ASTAR-811C	6
2. Effect of Cooling Conditions on Room Temperature Hardness of ASTAR-811C	5
3. Ductile-Brittle Transition Temperature of ASTAR-811C Sheet Tested in Bending	13
4. Bend Ductile-Brittle Transition Temperature for ASTAR-811C Sheet, GTA Welded Under Various Conditions	15
5. Effect of Post Weld Annealing on the Bend Ductile-Brittle Temperature of As-GTA Welded ASTAR-811C	15
6. Effect of Oxygen Contamination and Long Time Exposure at 1800 ^o F on the Bend Ductile Brittle Transition Temperature of ASTAR-811C	14
7. Tensile Properties of GTA Welded ASTAR-811C	22
8. The Effect of Final Annealing Temperature on the Room Temperature Tensile Properties of ASTAR-811C	29
9. Effect of Carbon on the Mechanical Properties of Tantalum Base Alloys	33
10. Analysis of Tantalum and Ta-10W Alloy Base Starting Material	37
11. Typical Chemical Analysis Results for Consumable and Non-Consumable Electrode Melted Ingots	40
12. Hardness Traverse Results for As-GTA Welded Tantalum Base Alloys	50
13. Effect of 1 Hour Post Weld Annealing on the Fusion and HAZ Hardness of As-GTA Welded Ta-8W-2Hf-0.05C	50
14. Room Temperature Tensile Properties of Tantalum Base Alloys Annealed 1 Hour at 3000 ^o F Prior to Test	58
15. Elevated Temperature Tensile Properties of Experimental Tantalum Alloy Sheet	61
16. Effect of Nitrogen on the 2400 ^o F Tensile Strength of Tantalum Alloys Tested in the As-Worked Condition	62
17. Effect of Rhenium on Properties of Ta-W-Hf-C Alloy	74

I. INTRODUCTION

The objective of this investigation was to develop a precipitation strengthened tantalum base alloy(s) for use in advanced Rankine cycle space nuclear power systems operating in the 2000-3000°F temperature regime. The alloys will be used as primary structural and liquid alkali metal containment materials in the form of sheet and tubing. Since the operational life of these systems is expected to be in excess of 10,000 hours, the resistance to creep deformation is the primary strength criterion. In addition to creep strength the alloys also must be fabricable, weldable, and resistant to liquid alkali metal corrosion.

This is believed to be the first refractory metal development program where primary emphasis was on optimizing long time creep properties. Heretofore, refractory metal alloy development programs have concentrated on improving short time tensile and stress rupture properties. It has indeed been a pleasant experience to have participated in such a highly successful alloy development program which has led to the discovery of the Ta-8W-1Re-0.7Hf-0.025C composition. This composition which has been designated ASTAR-811C, has significantly better long time creep properties than T-111 while still retaining fabricability and weldability characteristics comparable to those of T-111. This report will describe in detail the properties of ASTAR-811C and will also summarize the salient features of the investigative results from which evolved the Ta-8W-1Re-0.7Hf-0.025C (ASTAR-811C) composition. The experimental program which led to the development of ASTAR-811C is described in detail elsewhere.⁽¹⁾

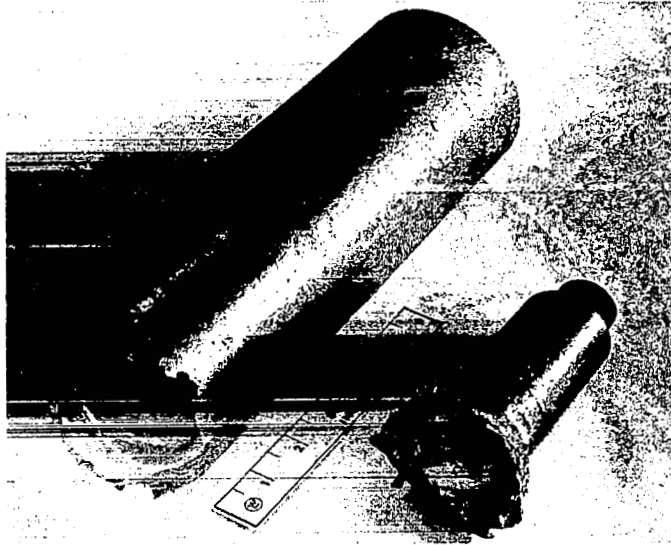
II. ASTAR-811C

ASTAR-811C is a tantalum base alloy containing 8% tungsten*, 1% rhenium, 0.7% hafnium and 0.025% carbon. Elevated temperature creep strength is achieved by a combination of solid solution and precipitate strengthening. The precipitating phase is a tantalum dimetal carbide (Ta_2C), which is dispersed in a tantalum matrix containing the tungsten, rhenium and hafnium in solid solution. Although from theoretical considerations hafnium would not be expected to make a significant contribution to improving the time dependent deformation properties, it is nevertheless required to impart liquid alkali metal corrosion resistance.

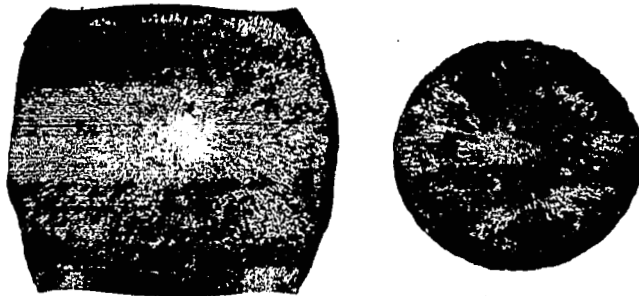
A. CONSOLIDATION

ASTAR-811C material for evaluation was prepared as 0.04 inch thick sheet from a double vacuum, consumable electrode arc melted 80 pound, 4 inch diameter ingot (heat NASV-20). The first melt electrodes were cast into a 2-1/2 inch diameter mold using a.c. power. The final melt into a 4 inch diameter mold was accomplished using d.c. power. The as-melted ingot was machine conditioned and processed to sheet utilizing processing procedures similar to those used for T-111 (Ta-8W-2Hf). This consisted of upset or side forging the as-cast ingot at 2200-2550°F using multiple blows on the Dynapak. The forging billets were protected from atmospheric contamination during heating and forging by an Al-12Si alloy coating. The as-forged ingot slabs were machine conditioned, annealed at 2550-3000°F for 1 to 2 hours and then warm rolled (500-800°F) to 1/4 inch thick plate. The as-rolled plate was annealed at 2550-3000°F for 1 to 2 hours and then rolled to 0.04 inch thick sheet at room temperature. Examples of the excellent workability of ASTAR-811C are illustrated in Figures 1 and 2 which show the as-melted ingot, upset and side forgings, as-rolled plate, and final as-rolled 18 inch wide x 33 inch long x 0.04 inch thick sheet. All processing was carefully controlled to ensure minimal contamination during hot breakdown and during intermediate and final annealing heat treatments.⁽¹⁾ The practices used were those which have been developed at WANL for processing columbium and tantalum base alloys with non-detectable amounts of contamination occurring during processing and testing. The results of this critical control which is exercised starting with the material going into the first melt electrode is evident from the

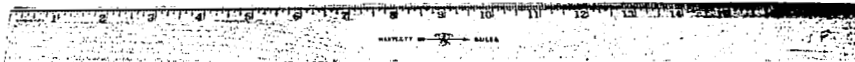
*Compositions given in weight percent.



(a) As-Melted Ingot



NASV
20



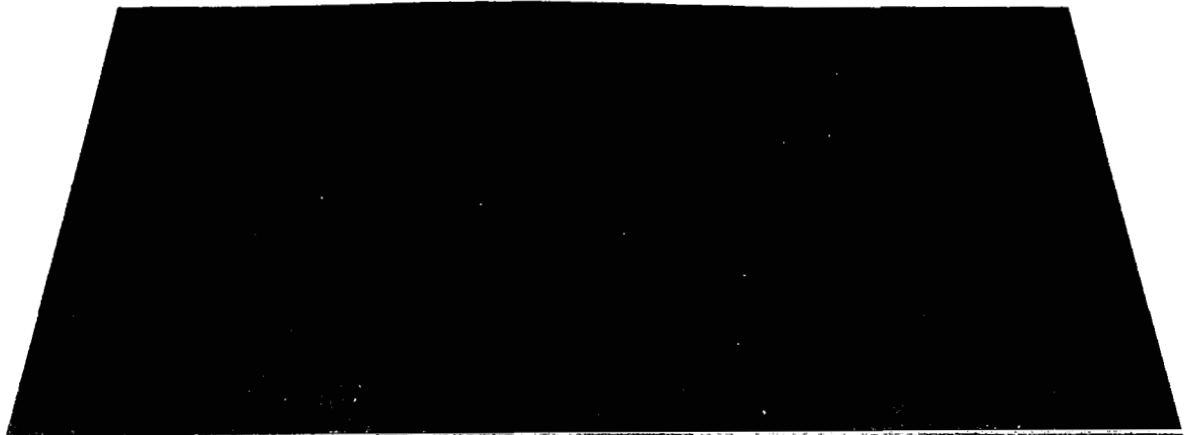
(b) Forgings

FIGURE 1 - As-Melted Ingot and As-Forged ASTAR-811C
(Heat NASV-20)



Metallurgical Laboratory

(a) 1/4" thick plate



Metallurgical Laboratory

(b) 0.04" thick plate

FIGURE 2 - As-Rolled 1/4" Thick Plate and 0.04" Thick Sheet of ASTAR-811C
(Heat NASV-20)

chemical analysis results presented in Table 1 for the as-melted ingot and as-annealed final sheet.

B. MICROSTRUCTURE

The microstructure of ASTAR-811C in the as-cast condition and at various stages during processing to 0.04 inch thick sheet is illustrated in Figure 3. Typically, the microstructure consists of tantalum dimetal carbide (Ta_2C) platelets dispersed throughout the single phase matrix. The Ta_2C forms a discontinuous precipitate growing from grain boundaries and also distributed uniformly throughout the grain volume. This form and distribution of the precipitate has no adverse effects on the workability of ASTAR-811C which is very similar to that of T-111.

C. RECRYSTALLIZATION BEHAVIOR

Heating cold worked Astar-811C sheet material at temperatures up to 2550°F results in softening and eventual formation of recrystallized grains. The isochronal annealing curve for sheet material given a prior cold reduction of 73% is illustrated in Figure 4. Formation of a completely equiaxed microstructure is complete after heating for one hour at 2550°F and better than 90% complete after one hour at 2400°F. The recrystallization behavior of ASTAR-811C is comparable to that of T-111. Although the rhenium and carbon additions have resulted in raising the hardness level, they did not apparently alter the recrystallization behavior significantly. Upon heating ASTAR-811C above 2500°F, there is a slight increase in room temperature hardness. This behavior is normally observed in carbon containing columbium and tantalum alloys and reflects the additional carbon taken into solution at the higher annealing temperatures and retained during subsequent cooling. Since the Ta_2C precipitates during cooling, the rate of cooling from annealing temperatures near or above the carbon solvus can significantly effect the room temperature hardness level as illustrated below in Table 2.

TABLE 2 - Effect of Cooling Conditions on Room Temperature Hardness of ASTAR-811C

Heated to 3630°F and furnace cooled	262 DPH
Heated to 3630°F and quenched by introducing He gas into chamber	290 DPH

TABLE 1 - Chemical Analysis Results for ASTAR-811C
(Heat NASV-20)

Sample Location	Analysis, weight percent					
	W	Re	Hf	C	O	N
Ingot Top	7.4	1.04	0.71	0.024	0.0006	0.0013
Ingot Bottom	7.2	0.92	1.01	0.023	0.0021	0.0027
0.04" sheet as- annealed 1 hr. at 3000°F	--	--	--	0.0200	0.0013	0.0020



150X



1500X

(a) As-Cast



(b) As Upset Forged (338 DPH)



(c) Upset Forged and Annealed
1 Hr. at 3000°F (258 DPH)



(d) As Rolled 1/4" Plate (365 DPH)



(e) 1/4" Plate, Annealed 1 Hr.
at 3000°F (249 DPH)

FIGURE 3 - Microstructure and Hardness of ASTAR-811C Mag. 500X



(f) As Rolled (76% Red.) 0.06"
Sheet (385 DPH)



(g) 0.04" Sheet, 33% Prior
Red. Annealed 1 Hr. at
3000°F (249 DPH)

FIGURE 3 (Continued) - Microstructure and Hardness of ASTAR-811C Mag. 500X

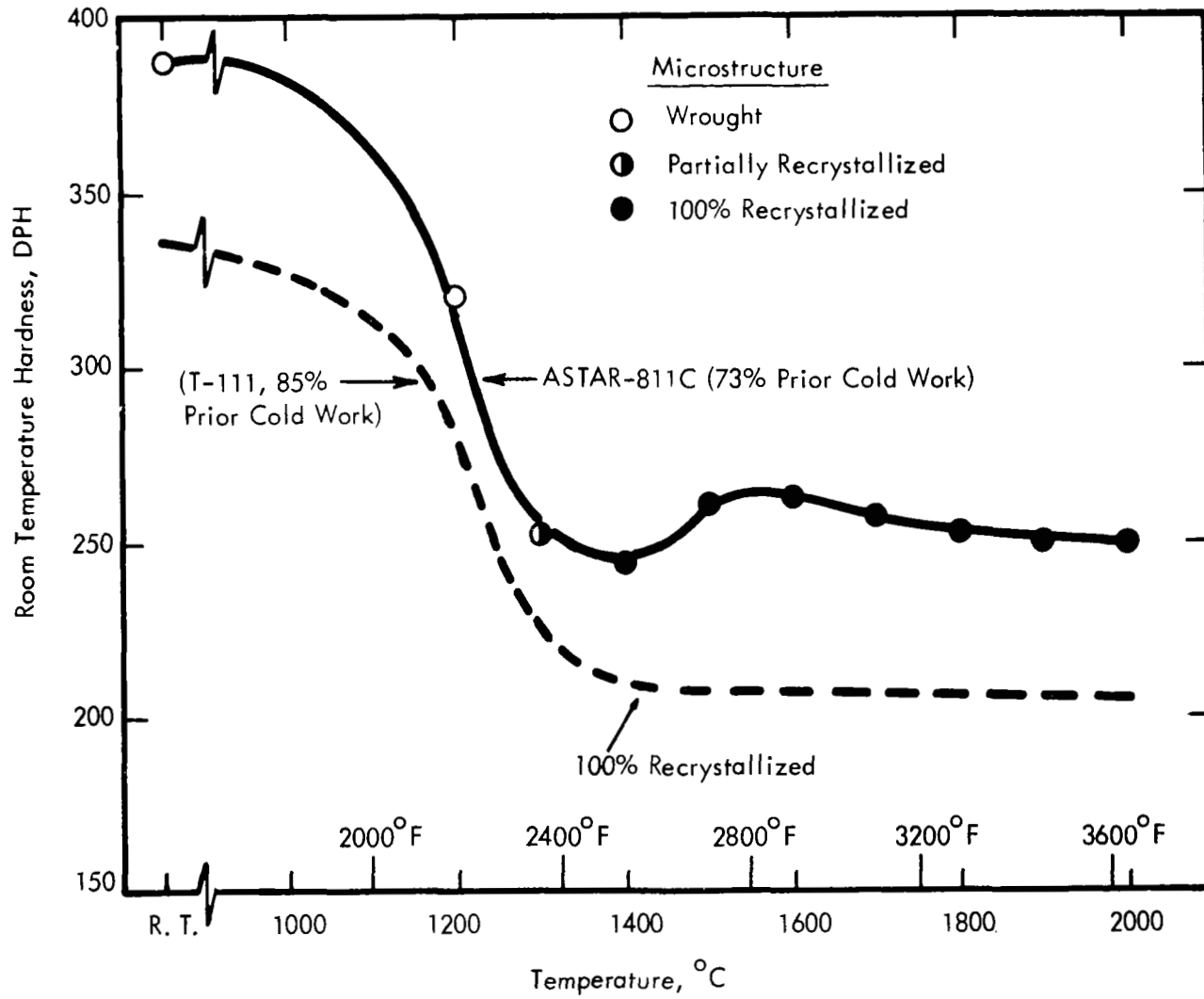


FIGURE 4 - Recrystallization Behavior of ASTAR-811C

As rhenium and carbon did not appear to significantly alter the recovery and recrystallization behavior of ASTAR-811C from that of T-111, neither did these additions alter the recrystallized grain size. The recrystallized grain size of ASTAR-811C after heating for 1 hour at 3000°F was normally ASTM 7-8 and is the same grain size exhibited by comparably cold worked T-111 sheet annealed 1 hour at 3000°F. Increasing the amount of cold work generally resulted in a finer as-recrystallized grain size when heating the as-worked sheet at 3100°F and lower (See Figure 5). However, when heating the as-worked sheet at temperatures in excess of 3100°F, the final grain diameter after 1 hour was little influenced by the amount of prior work. This of course reflects the significant contribution of grain growth to the final grain size during the isochronal treatments at temperatures above 3100°F. This is illustrated in the isothermal annealing curves shown in Figure 6 where the rate of growth is shown to be very low at temperatures below 3100°F.

D. WELDABILITY

One of the prime features of ASTAR-811C is the retention of good as-welded ductility concomitant with a significant improvement in creep strength. ASTAR-811C sheet, 0.04 inch thick, was welded by the tungsten arc-inert-gas (GTA) and electron beam techniques and then tested in bending with the weld bead transverse to the bend axis over a nominal bend radius of 0.04 inch (1t bend factor). Testing was accomplished at lower and lower temperatures until the specimen fractured before sustaining a full 90° bend. All sheet material was annealed for one hour at 3000°F prior to welding. The weld beads were not conditioned nor treated in any manner after welding. The top of the weld bead was the tension side of the specimen. GTA welding was done under a controlled high purity helium atmosphere and electron beam welding was done in a chamber which had been evacuated to less than 5×10^{-6} torr. Description of the welding conditions are detailed elsewhere.⁽¹⁾ As can be seen in Table 3, the bend ductility of ASTAR-811C was unaffected by electron beam welding and only slightly decreased by GTA welding. During welding, all or most of the carbide precipitate goes into solid solution in the fusion and heat affected zone. Subsequent cooling is rapid enough to suppress reprecipitation, thus significantly increasing the room temperature hardness with a

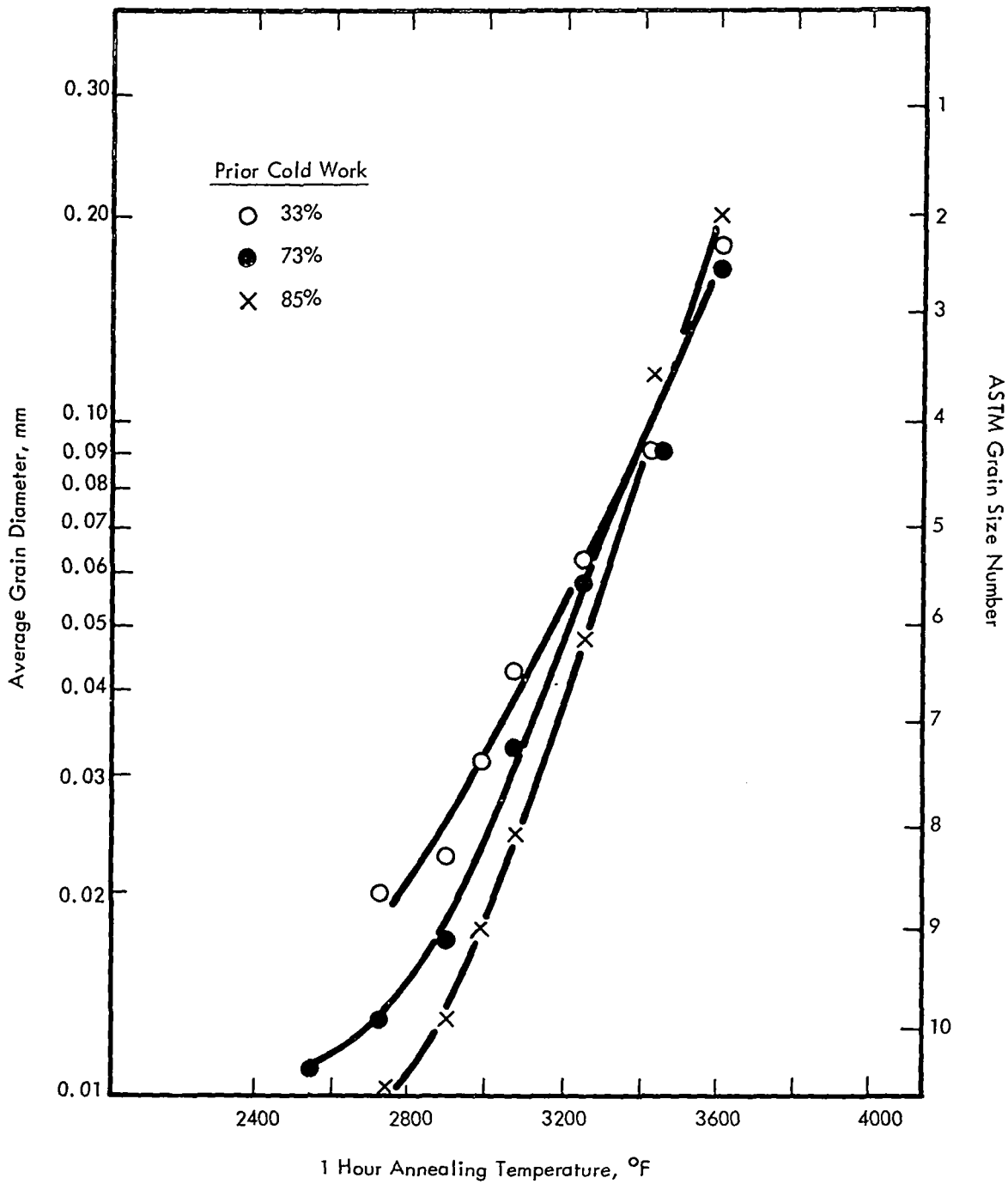


FIGURE 5 - Recrystallization Behavior of ASTAR-811C
(Heat NASV-20)

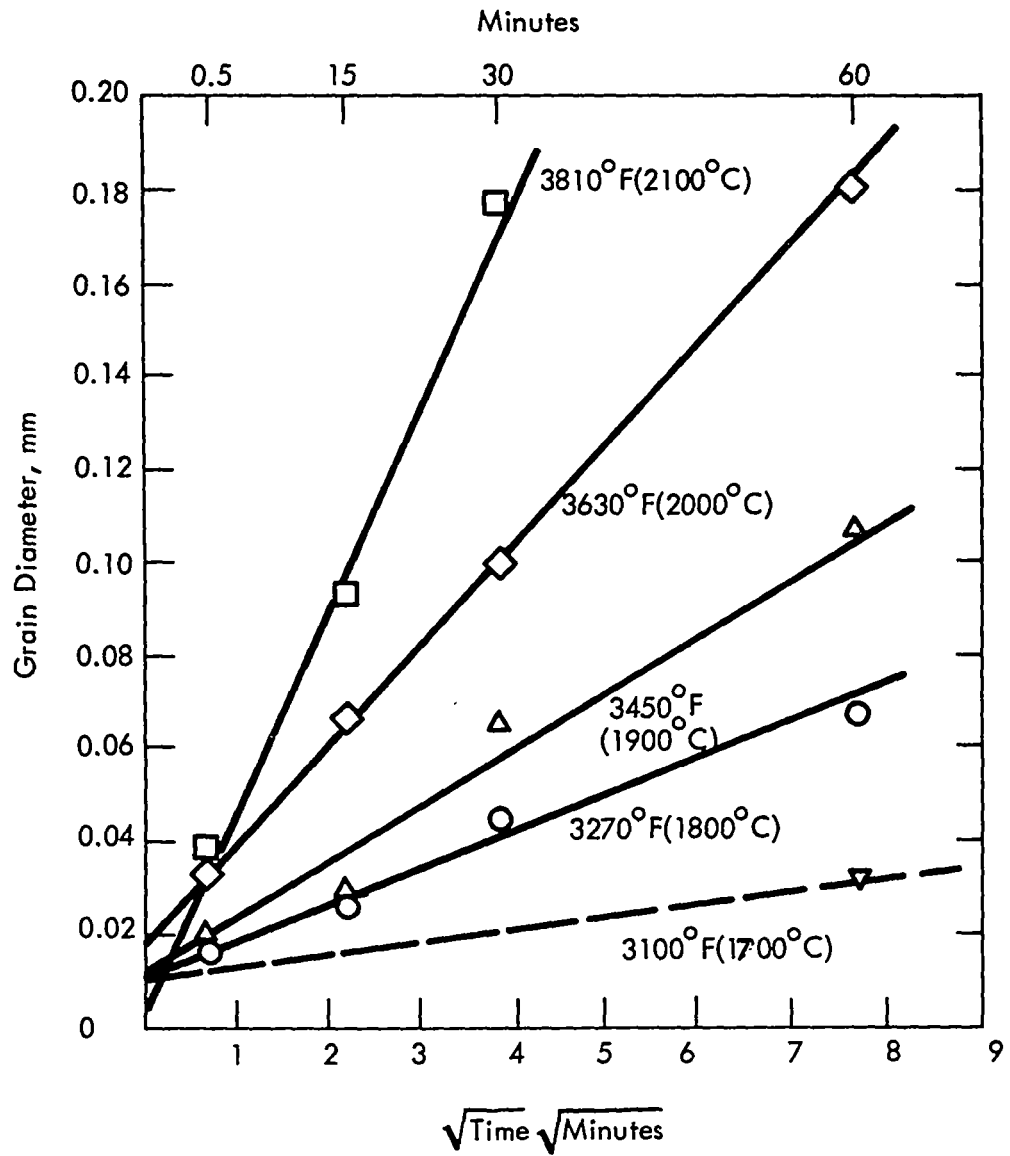


FIGURE 6 - Isothermal Annealing Curves for ASTAR-811C Sheet

TABLE 3 - Ductile-Brittle Transition Temperature of ASTAR-811C Sheet,
Tested in Bending

Condition ^(a)	DBTT	
	°F	°C
Base Metal	<-320	<-195
As-Electron Beam Welded	<-320	<-195
As-GTA Welded	-175 to -250	-155 to -157

(a) 0.04 inch sheet, annealed for 1 hour at 3000°F prior to welding and/or testing.

resulting increase in the bend ductile-brittle transition temperature. A hardness traverse and typical microstructures from a transverse section of a GTA weld are shown in Figure 7. ASTAR-811C can be GTA welded under a variety of conditions and still exhibit good weld metal ductility as determined by the bend test as shown by the data in Table 4. Likewise, post weld annealing as-GTA welded ASTAR-811C for times up to 10 hours over the temperature range of 2200-2400°F does not significantly alter the bend ductile-brittle transition temperature (See Table 5).

E. THERMAL STABILITY AND EFFECT OF OXYGEN CONTAMINATION

One of the critical properties of refractory materials being used in advanced space power systems is the ability of weldments to withstand long time thermal exposure without degradation of ductility. They should also be able to sustain a moderate amount of oxygen contamination during accidental atmospheric exposure during testing in earth bound environmental chambers without incurring serious loss of ductility. This is an area of investigation which was studied in limited detail on ASTAR-811C sheet material. As-GTA welded and as-annealed base metal were exposed for 1000 hours at 1800°F without suffering a significant loss in bend ductility. ASTAR-811C sheet material was also intentionally contaminated with oxygen prior to GTA welding. The contaminated and welded material was then exposed for 1000 hours at 1800°F. Material contaminated with 150 ppm O₂ suffered only a moderate loss of bend ductility. The data on the GTA welded and oxygen contaminated material are presented in Table 6.

TABLE 6 - Effect of Oxygen Contamination and Long Time Exposure at 1800°F on the Bend Ductile Brittle Transition Temperature of ASTAR-811C

Bend Ductile Brittle Transition Temperature, °F						
Base Metal	O ₂ Contaminated and then GTA Welded			O ₂ Contaminated, GTA Welded plus 1000 hrs. at 1800°F		
	None	150 ppm	350 ppm	None	150 ppm	350 ppm
-320	-250	+75	+250	-100	---	+200

TABLE 4 - Bend Ductile-Brittle Transition Temperature for ASTAR-811C Sheet, GTA Welded Under Various Conditions

DBTT, °F, for Narrow ^(a) GTA Welds for Welding Parameters of			DBTT, °F, for Wide ^(b) GTA Welds for Welding Parameters of		
7.5 ipm 76 amps	15 ipm 80 amps	30 ipm 124 amps	7.5 ipm 103 amps	15 ipm 118 amps	30 ipm 158 amps
-200	<-250	<-250	-250	-175	-200

- (a) Narrow GTA welds taper from 0.1 to 0.14 inches at top to 0 to 0.009 inches at bottom.
- (b) Wide GTA welds taper from 0.16 to 0.2 inches at top to 0.11 to 0.19 inches at bottom.

TABLE 5 - Effect of Post Weld Annealing on the Bend Ductile-Brittle Temperature of As-GTAWelded ASTAR-811C

Bend Ductile-Brittle Transition Temperature, °F, After Post Weld Annealing of:			
As-Welded	2 Hrs. at 2200°F	2 Hrs. at 2400°F	10 Hrs. at 2400°F
<-250	<-175	<-200	<-200

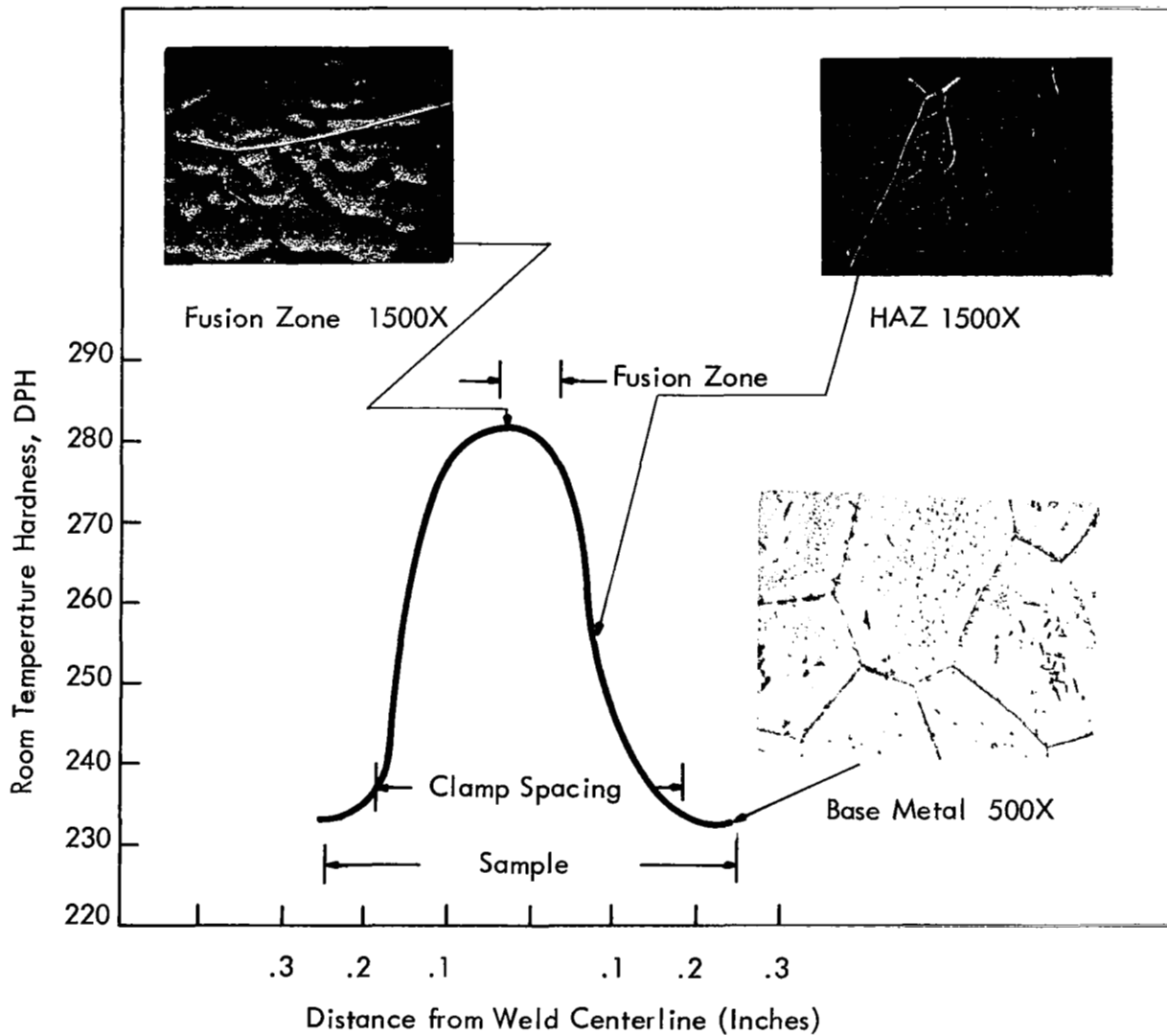


FIGURE 7 - Hardness Traverse and Microstructure of TIG Welded 0.04" Thick ASTAR-811C

Hardness traverses across transverse weld sections taken from specimens which had been oxygen contaminated and welded, oxygen contaminated, welded and aged, and welded and aged are presented in Figure 8. Microstructures from selected areas of the contaminated and welded and aged ASTAR-811C specimens are shown in Figure 9. The letter notations on the hardness traverse plot in Figure 8 corresponds to the area from which the photomicrographs of Figure 9 were taken. As will be discussed in more detail later, the only precipitating carbide phase in ASTAR-811C is the tantalum dimetal carbide Ta_2C and occurs by the following reaction:



Carbon precipitates from solid solution as Ta_2C and this results in a lowering of the hardness of the matrix.⁽¹⁾ Conversely, intentional oxygen contamination at temperatures of 1800°F (980°C) and less resulted in the formation of a coherent HfO_2 ppt which causes an increase in hardness of the matrix. At temperatures above 2000°F (1100°C) loss of coherency of the HfO_2 precipitate occurs very rapidly.⁽²⁾ However, at 1800°F (980°C), the loss of coherency occurs at a much lower rate. The kinetics of the reaction have yet to be studied in any great detail since the temperature range in which the oxide strengthening is the greatest is of little interest for application of tantalum base alloys. The study of the thermal stability and contamination behavior at ASTAR-811C was limited and is an investigative area where much remains to be done.

F. MECHANICAL PROPERTIES

1. Tensile Properties

a. Base Metal. The tensile properties of ASTAR-811C over the range of -320°F to 2800°F are plotted in Figure 10. ASTAR-811C exhibits excellent low temperature ductility and is essentially identical to that exhibited by T-111. The tensile yield and ultimate strength of ASTAR-811C is about 10% greater than T-111. Thus from a comparison of tensile strength, ASTAR-811C can be considered as a moderate strength alloy.

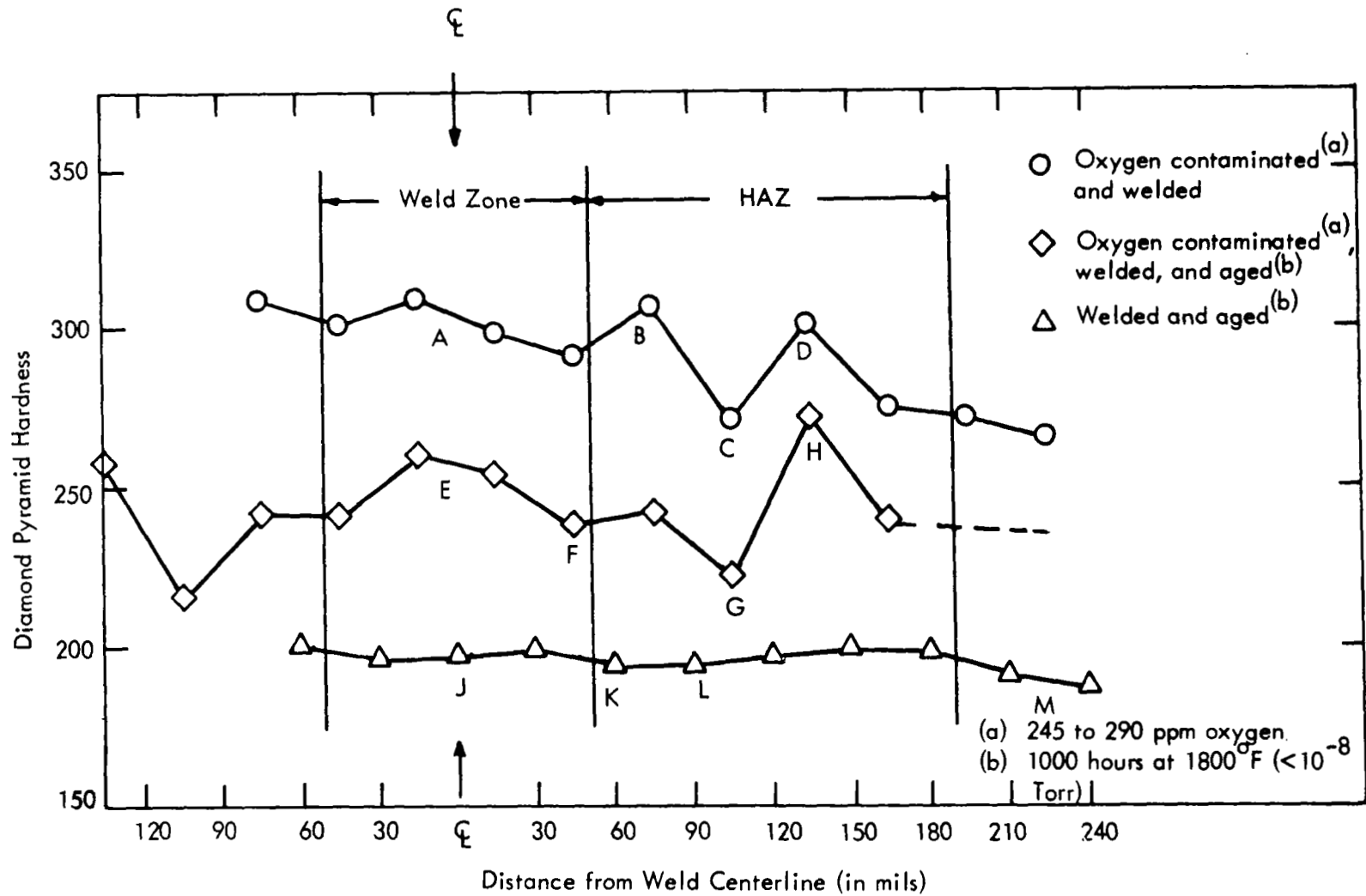
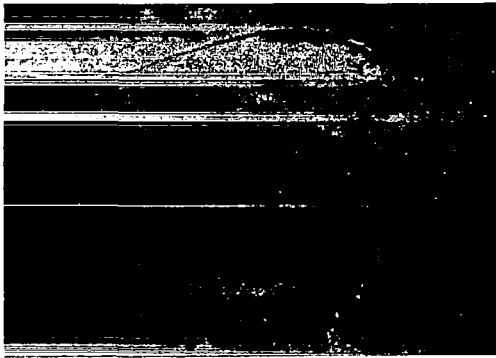
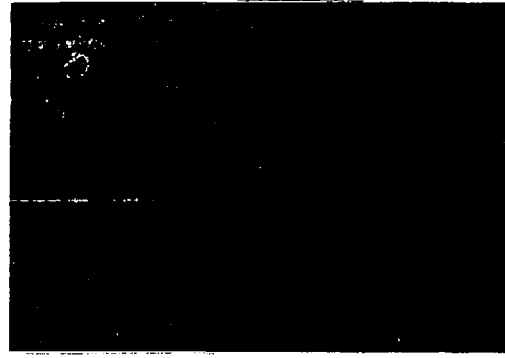


FIGURE 8 - Hardness Traverse for ASTAR-811C Weld Specimens

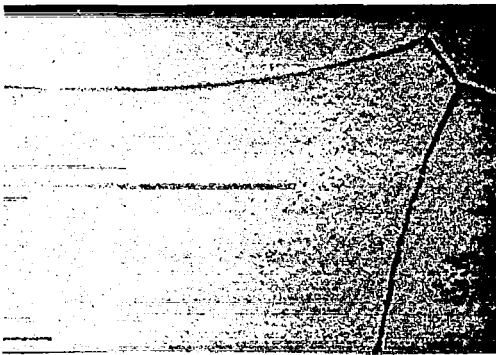


(a) Weld Zone (Point A in Fig. 8) 1500X
305 DPH

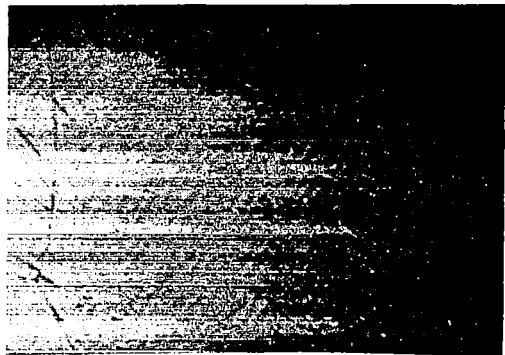


(b) HAZ (Point B in Fig. 8) 1500X
305 DPH

Oxygen Contaminated and Welded Specimen



(c) HAZ (Point C in Fig. 8) 1500X
270 DPH

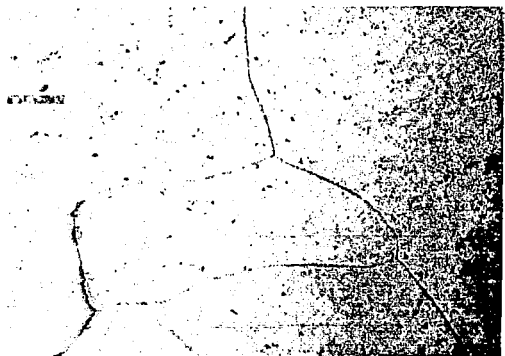


(d) HAZ (Point D in Fig. 8) 1500X
300 DPH

Oxygen Contaminated and Welded Specimen



(e) Weld Zone (Point E in Fig. 8) 500X
255 DPH



(f) Weld Zone (Point F in Fig. 8) 500X
262 DPH

Oxygen Contaminated, Welded, and Aged^(a) Specimen
(a) 1000 Hrs. at 1800°F ($<10^{-8}$ Torr)

FIGURE 9 - Microstructure of ASTAR-811C (Heat NASV-20) Welded Specimens

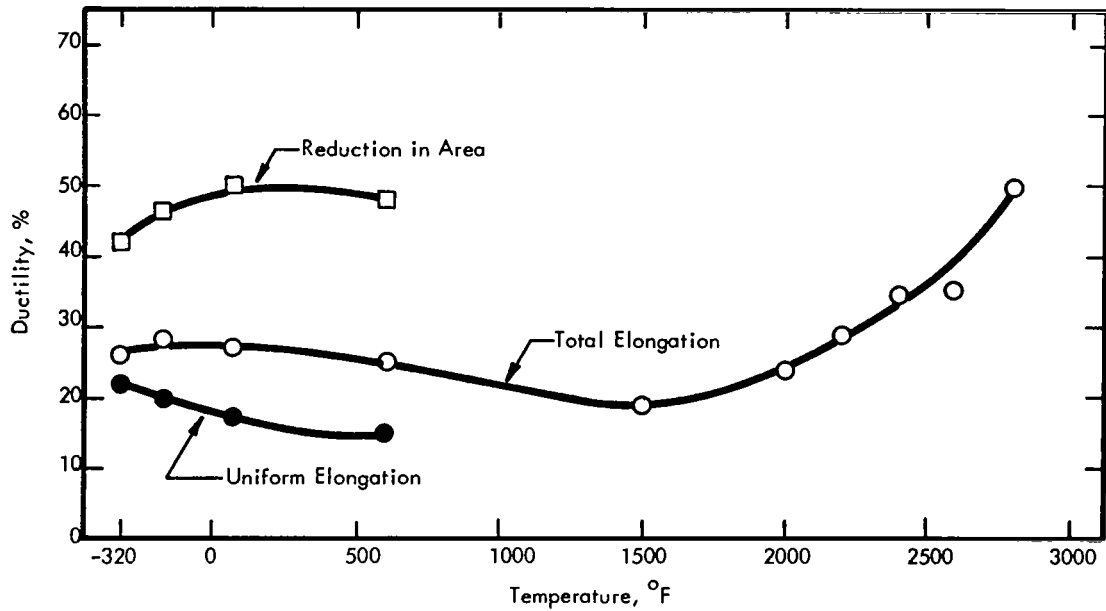
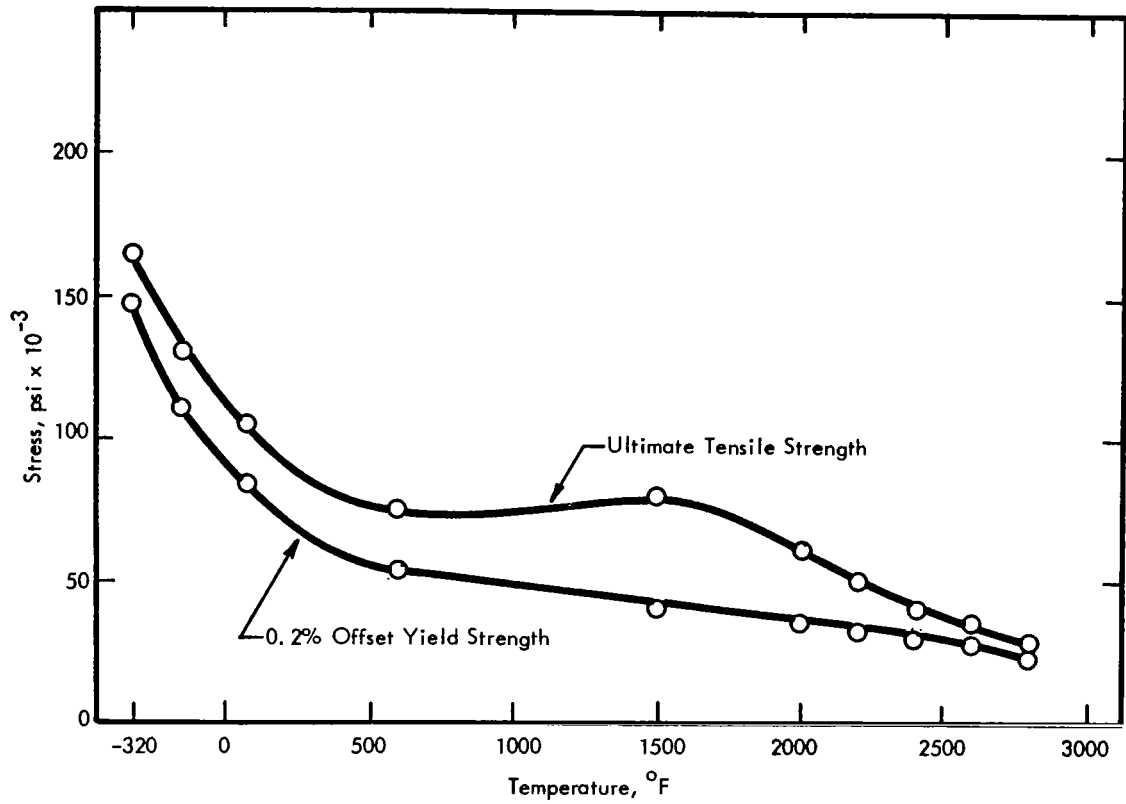


FIGURE 10 - Tensile Properties of ASTAR-811C (Heat NASV-20). (Tests Performed on 0.04 inch sheet, annealed 1 hour at 3000°F prior to testing at a constant strain rate of 0.05 in/min).

b. Weld Metal. The tensile properties of GTA weldments determined over the same temperature range as for the base sheet material are summarized in Table 7. The tensile yield and ultimate tensile strength of the GTA weldments are compared with the base metal in Figure 11. The somewhat higher tensile strength of the weldments is caused by the solutioning of the carbon during welding as discussed earlier. The strengthening contribution of carbon in solid solution is effective at room temperature and below but at elevated temperatures, the carbide precipitation reaction is sufficiently rapid to minimize any contribution of the solid solution strengthening of the carbon to the elevated temperature strength.

2. Creep Properties

Improving the time dependent behavior characteristics of tantalum while still retaining the desirable characteristics of good weldability, fabricability, and good low temperature ductility were the primary aims of the research program which led to the development of ASTAR-811C. A comparison of the creep behavior of ASTAR-811C with that of T-111 is illustrated in the plot of Figure 12. The time to elongate 1% is the creep parameter used as the basis for comparison and is normalized using the Larson-Miller parametric plot. At 2400°F, the stress required to elongate ASTAR-811C, 1% in 1000 hours is 2-1/2 times greater than that required for T-111. This is a significant improvement when considering that the tensile strength of ASTAR-811C is only 10% greater than that of T-111. The data in Figure 12 are from tests on 0.04 inch thick sheet material annealed 1 hour at 3000°F prior to test. All creep testing was done under ultra high vacuum conditions, i.e., test pressure $\leq 1 \times 10^{-8}$ torr, to inhibit test environment-test specimen interactions which could result in generation of spurious test data. (3) However, time dependent deformation properties are sensitive to a number of factors which include grain size, annealing temperature, and metallurgical condition which is a function of the prior thermal-mechanical history.

TABLE 7 - Tensile Properties of GTAWelded ASTAR-811C^(a)

Test Temp. (°F)	Weld Direction	0.2% Yield Strength (psi)	Ultimate Tensile Strength(psi)	% Elongation		% Reduction in Area
				Uniform	Total	
-320	Longitudinal	157,300	184,600	16.65	24.20	35.65
-320	Transverse	159,000	176,200	10.90	14.15	41.10
RT	Longitudinal	109,800	115,300	15.0	28.45	48.90
RT	Transverse	89,300	107,200	10.6	18.7	47.8
1800	Longitudinal	44,000	67,100	--	18.7	--
2400	Longitudinal	35,300	41,100	--	29.0	--
2600	Longitudinal	32,500	36,000	--	26.7	--

(a) A constant strain rate of 0.05 inches/minutes used throughout the test. All material tested in the as-welded condition.

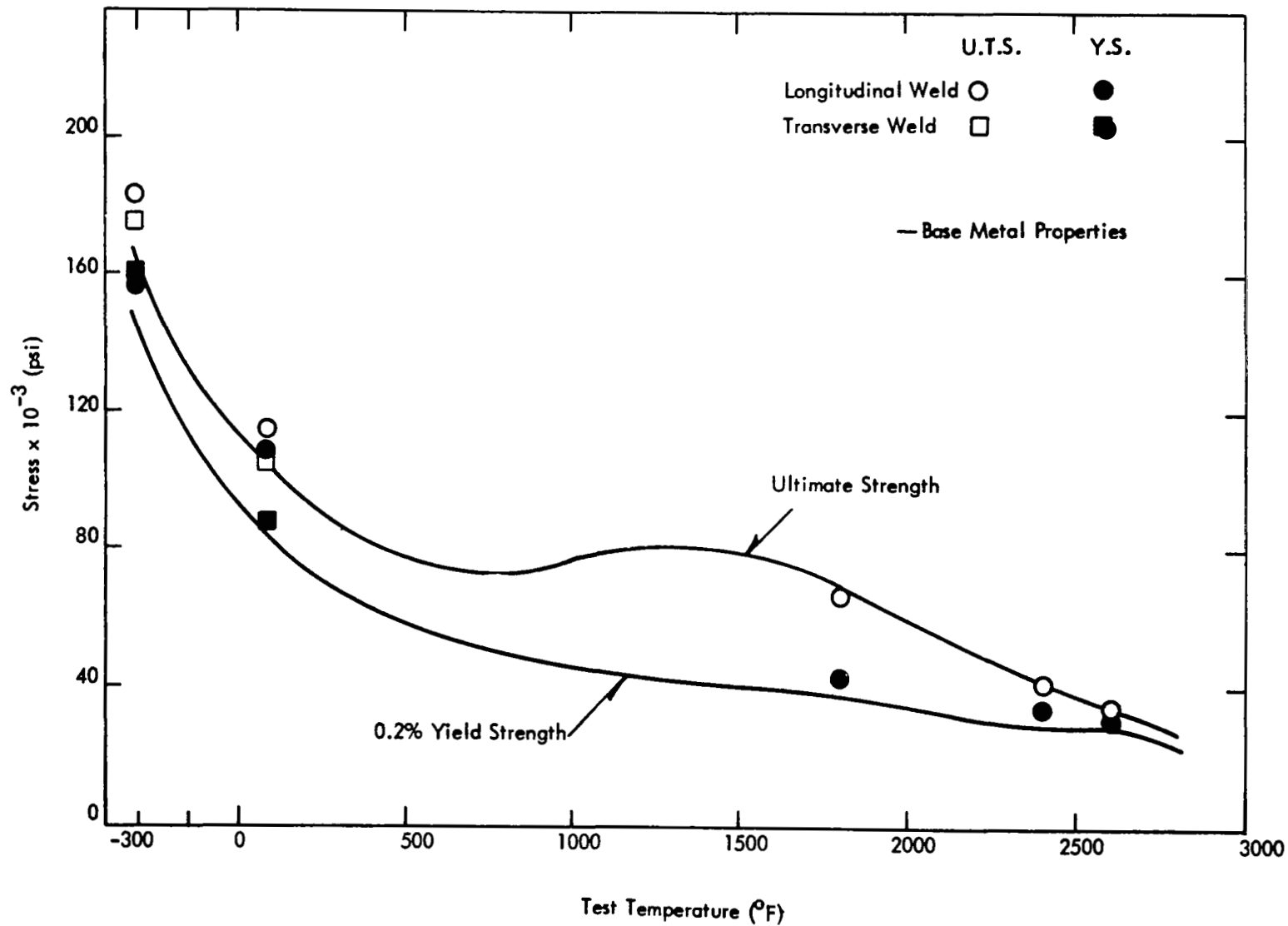


FIGURE 11 - Tensile Properties of GTA Welded ASTAR-811C Compared with that of 0.04 Inch Sheet

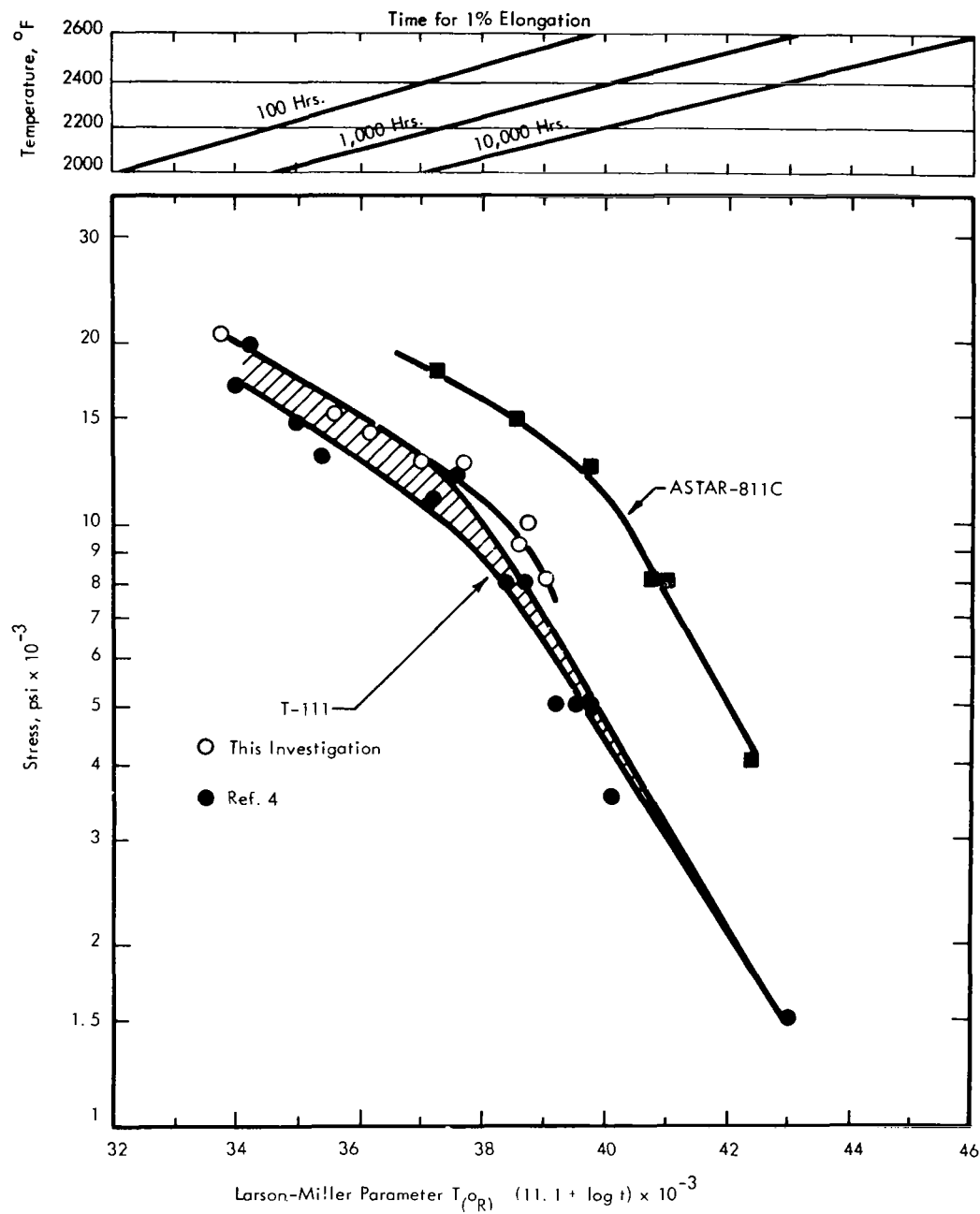


FIGURE 12 - Creep Properties of ASTAR-811C Compared to T-111 on Parametric Plot of Time to Elongate 1%. (All material annealed 1 hour at 3000°F prior to test).

a. Response to Heat Treatment. ASTAR-811C is a relatively complex high temperature alloy which contains a carbide phase that exhibits a solubility relationship with the matrix. A wide range of creep properties can be achieved by altering the final thermal treatment. For example, increasing the final annealing temperature from 3000°F to 3630°F results in approximately doubling the time to elongate 1% at 2400°F at an applied stress of 15,000 psi (See Figure 13). Of course, the increase in annealing temperature resulted in a coarsening of the as-recrystallized grain size from 0.03 mm to 0.2 mm, and grain size is known to exert an influence on the creep behavior.⁽⁵⁾ Accompanying this grain growth with increasing annealing temperature is a change in the Ta₂C (dimetal carbide) morphology which is illustrated in the transmission electron micrographs of Figure 14. However, the limited experimentation that was conducted to isolate the individual contributions of the grain size, and final annealing temperature on the creep properties of ASTAR-811C were not conclusive. The data plotted in Figure 15a shows that when ASTAR-811C is tested at 2400°F and 15,000 psi, the creep behavior is independent of final annealing temperature at a grain size of 0.03 mm. However at a grain size of 0.07 mm, the creep behavior is strongly influenced by the final annealing temperature. Annealing at 3630°F has the most significant effect on the creep properties and as seen in Figure 15b, there appears to be an optimum grain size for improved creep resistance. An optimum grain size for creep has been previously found for nickel and iron base alloys⁽⁵⁾.

Increasing the annealing temperature also raises the room temperature properties. (See Table 8 and Figure 16). After annealing for one hour at 3630°F (2000°C) and cooling rapidly, the microstructure of ASTAR-811C appears single phase when viewed optically. However, when viewed by transmission electron microscopy the presence of a fine precipitate which exhibited coherency strain to some degree with the matrix, was observed (See Figure 17). Even though initially there appears to be coherency of the Ta₂C precipitate with the matrix, the kinetics of the precipitation reaction at elevated temperature are rapid and coherency is short lived. The finely divided non-coherent Ta₂C does appear to offer obstacles to dislocations. (See Figure 18).

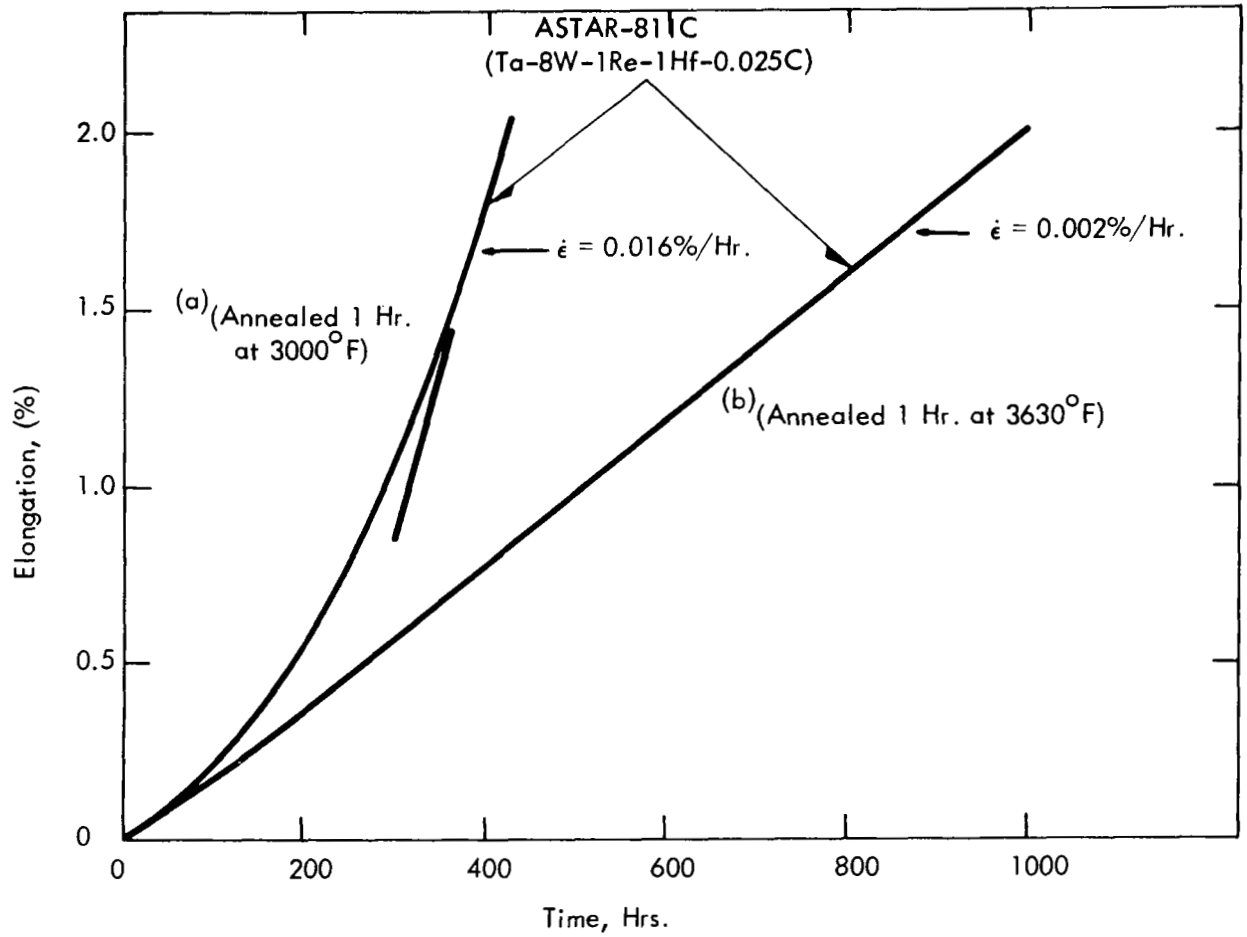


FIGURE 13 - Effect of Final Annealing Temperature on the Shape of the Creep Curve for ASTAR-811C Tested at 2400°F and 15,000 psi



(a) One Hr. at 3000°F (1650°C)
(Test Time - 500 Hrs.)



(b) One Hr. at 3270°F (1800°C)
(Test Time - 500 Hrs.)



(c) One Hr. at 3630°F (2000°C)
(Test Time - 1000 Hrs.)

FIGURE 14 - Electron Micrographs Showing Effect of Final Annealing Temperature on the Carbide Morphology. (All residues extracted from gage length of creep specimens after testing at 2400°F, 15,000 psi, test time noted).
Mag. 3000X

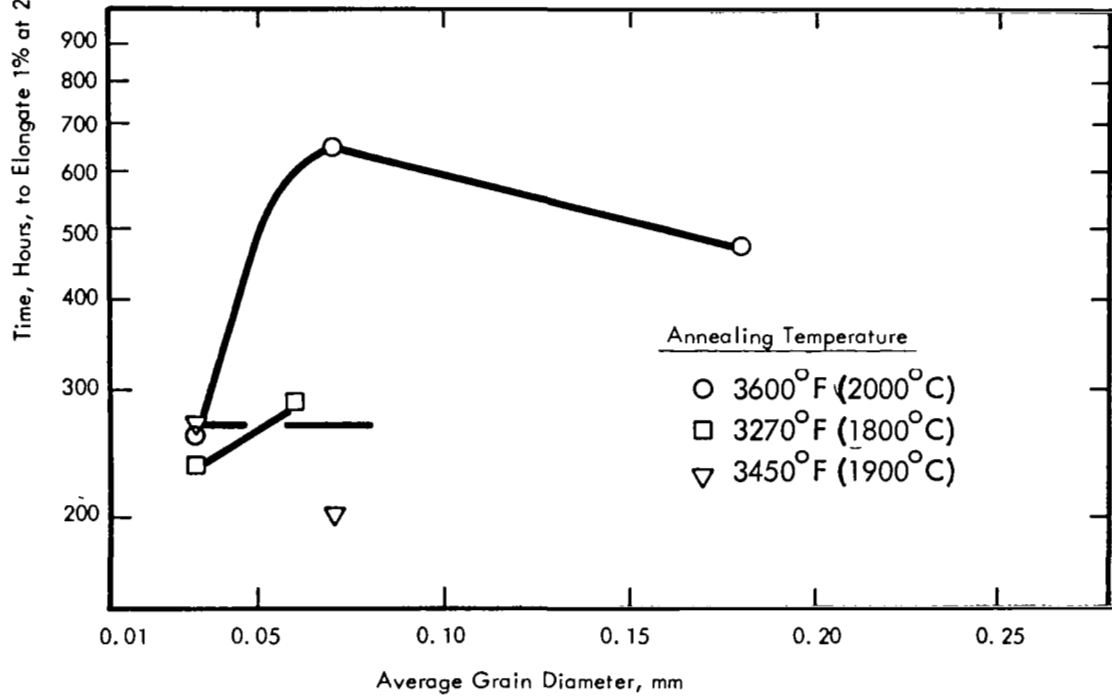
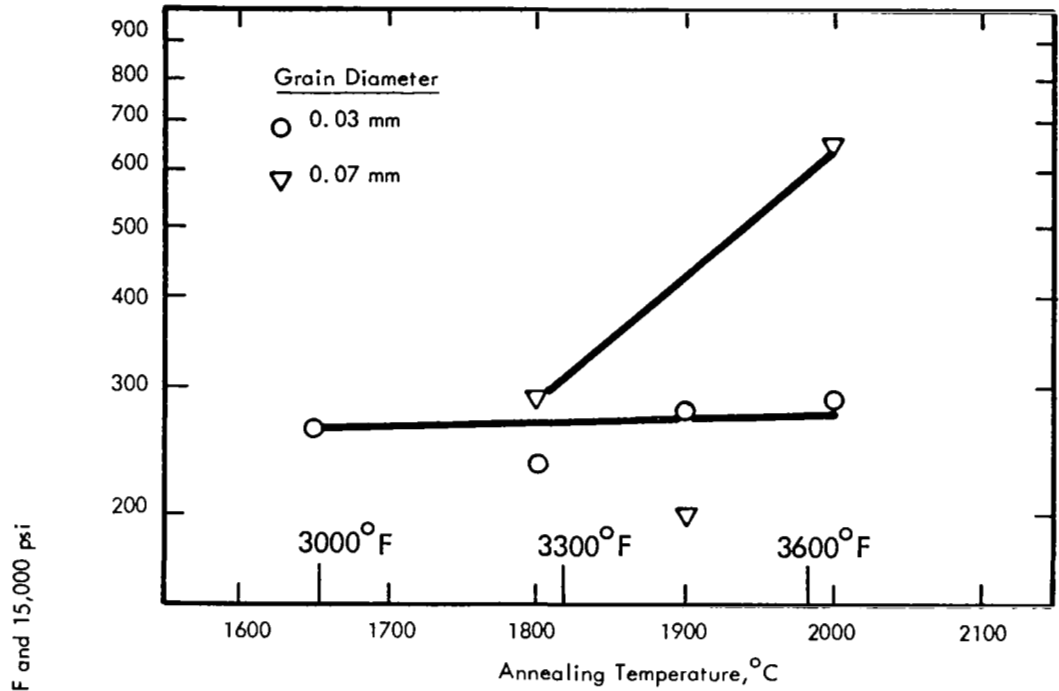


FIGURE 15 - Effect of Grain Size and Final Annealing Temperature on Creep Properties of ASTAR-811C

TABLE 8 - The Effect of Final Annealing Temperature on the Room Temperature Tensile Properties of ASTAR-811C

Pre-test Heat Treatment (°F)	0.2% Yield Strength (psi)	Ultimate Tensile Strength (psi)	% Elongation		% Reduction in Area	Proportional Limit (psi)	DPH	Grain Size (mm)
			Uniform	Total				
1 hr/3000°F furnace cool	83,400	105,400	16.2	24.8	51.9	74,300	258	0.020
1 hr/3270°F furnace cool	84,300	104,600	15.8	23.1	49.2	79,000	260	0.050
1 hr/3630°F furnace cool	90,000	105,300	16.2	23.2	44.7	83,700	262	0.180
1 hr/3810°F furnace cool	103,200	105,000	9.9	18.4	38.4	94,000	279	0.400
1 hr/3630°F helium quench	102,700	108,800	10.8	17.0	46.4	97,600	289	~ 0.180

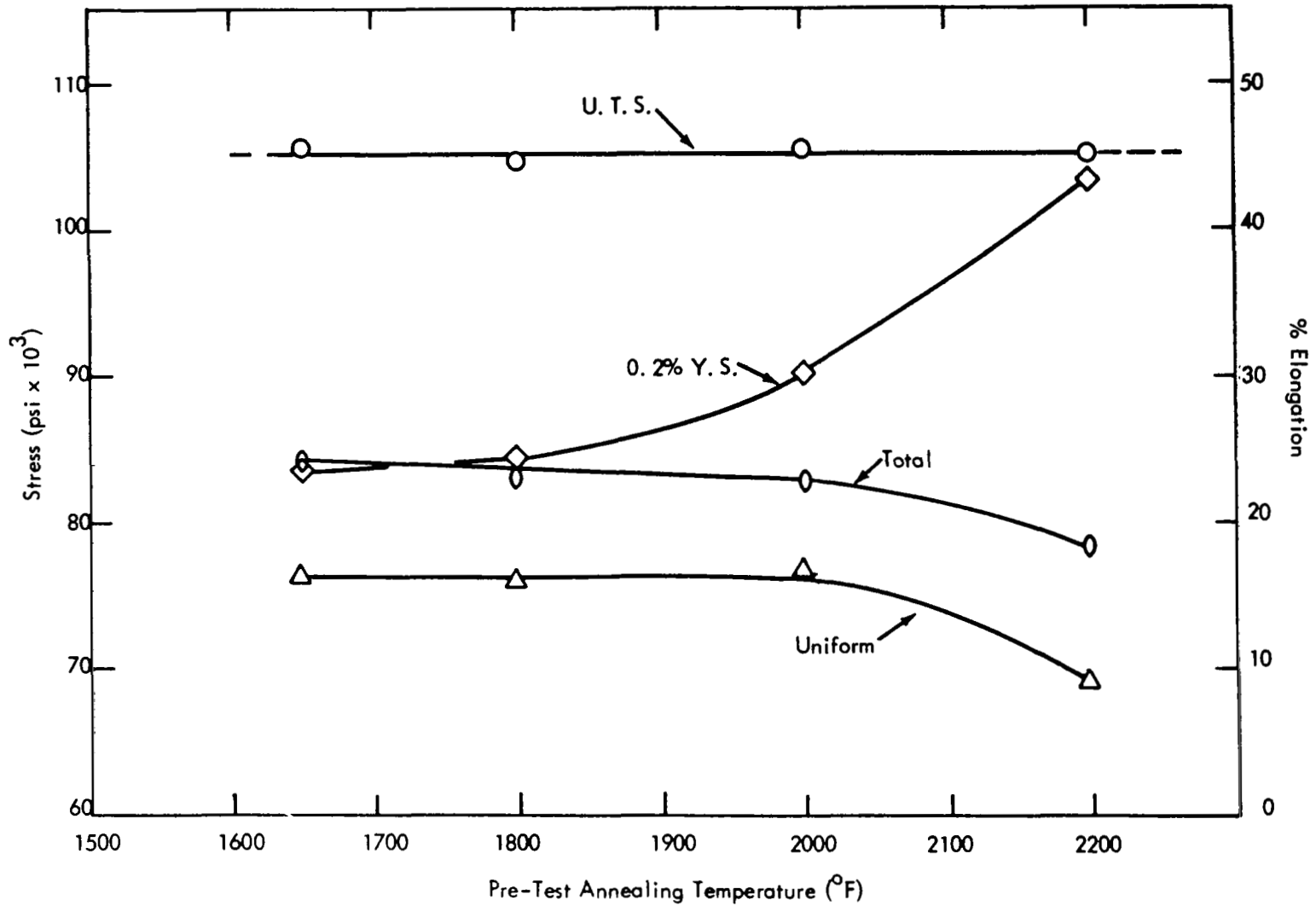
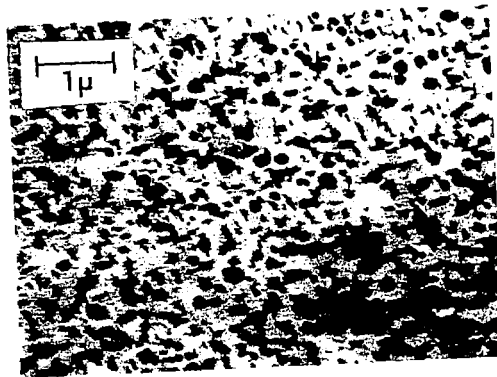


FIGURE 16 - Effect of Final Annealing Temperature on the R. T. Tensile Properties of ASTAR-811C



(a)



(b)

FIGURE 17 - Electron Transmission Photomicrograph of ASTAR-811C Sheet, Annealed One Hour at 3630^oF and Rapidly Cooled. (a) Interior of Grain (b) Grain Boundary.



FIGURE 18 - Transmission Electron Micrograph of ASTAR-811C Sheet, Annealed One Hour at 3630°F (2000°C), Rapidly Cooled, then Creep Tested at 2400°F and 15,000 psi at $<1 \times 10^{-8}$ torr. Test Duration 1000 Hrs., Total Creep Elongation 2.5%.

Although the exact mechanism(s) by which carbides confer elevated temperature strength on ASTAR-811C have not as yet been identified, the potency of the carbon addition on creep strength is illustrated by the data in Table 9.

TABLE 9. Effect of Carbon on the Mechanical Properties of Tantalum Base Alloys

Property	Ta-8W-1Re-1Hf	ASTAR-811C (Ta-8W-1Re-1Hf-0.025C)
Tensile Strength		
Room Temperature	88,000 psi	105,000 psi
2400°F	34,000 psi	41,000 psi
Creep Properties		
Time to 1% Strain		
at 2400°F, 15,000 psi	54 hrs.	260 hrs.

The comparison is in Table 9 for sheet material annealed 1 hour at 3000°F prior to test. The Ta-8W-1Re-1Hf alloy contained less than 20 ppm carbon and less than 50 ppm C+O₂+N₂. The strengthening effect of carbon is diminished as the test temperature is increased and the contribution of carbon to the creep strength is negligible above 2600°F.

There is a large amount of testing required yet to fully define the creep properties of ASTAR-811C and the effects of heat treatment, metallurgical structure, and final grain size on these properties.

b. Phase Relationships

The only precipitating phase found in ASTAR-811C is the (Ta₂C) tantalum dimetal carbide. This has been the only phase found after heating for times up to 1000 hours at temperatures up to 3000°F. The carbon solvus for ASTAR-811C has been determined to occur at about 3600°F. At this temperature all of the 250 ppm carbon is in solid solution. More elegant heating and quenching experiments will have to be devised since the rapid precipita-

tion kinetics of the Ta_2C necessitate cooling rates in excess of $40F^{\circ}/sec$ to suppress the precipitation of Ta_2C . As discussed earlier, the morphology of the Ta_2C precipitate can be significantly altered by heat treatment. This feature provides an additional means of controlling the final mechanical properties. Although ASTAR-811C contains W, Re and Hf, no Re and only minor amounts of W and Hf have been detected in the Ta_2C precipitate.

III. ALLOYING EFFECTS IN TANTALUM

Leading to discovery of the ASTAR-811C composition was a systematic study of the Ta-W-Hf-C system. The Ta-W-Hf system had been investigated previously⁽⁶⁻¹⁰⁾ and alloy compositions within this system exhibited good elevated temperature strength and fabricability. The utilization of transition metal carbides as a dispersed phase strengthener was demonstrated by Ammon and Begley⁽¹⁰⁾ in the development of T-222 (Ta-10W-2.5Hf-0.01C) and has also been used effectively in strengthening columbium base alloys^(11,12). Thus strengthening of the experimental tantalum base alloys was to be achieved by combination of solid solution plus dispersed phase strengthening. The dispersed second phase was to be achieved by the interaction of Hf and/or Zr with C and/or N.

Although no theory permitted an explicit quantitative prediction of compositions which would have optimum creep strength, the main factors which influence the creep behavior of a single phase matrix containing a stable dispersed second phase were defined using the model proposed by Ansel⁽¹³⁾ and Weertman⁽¹⁴⁾. Basically, this rationale limits alloying additions to those which would (1) decrease the diffusivity of the matrix and (2) increase the shear modulus of the matrix. Since creep is a diffusion controlled process, the matrix element strongly limits strength improvement to be achieved by alloying.

A. EXPERIMENTAL PROGRAM DESIGN

Tantalum alloys investigated within the Ta-W-Hf-C system had a compositional range of 3-15%W, 0.5-3.9%Hf, and 0.02-0.3%C. The effect of a partial substitution of Re and Mo for W, Zr for Hf, and N for C was studied using the following four base compositions:

Ta-8.6W-0.53Hf-0.02C

Ta-8.6W-0.53Hf-0.035C

Ta-8.2W-1Hf-0.035C

Ta-8.2W-1Hf-0.070C

Substitution of up to 1.5%Re, 0.85%Mo, 0.5%Zr, and 0.08%N were studied using a statistical design of 1/4 replication. Alloy compositions containing up to 3% Re were also investigated. Although molybdenum was not considered to be as an effective addition as tungsten for improving creep strength, it may affect the carbide/nitride solubility relationship and interfacial energy between the precipitate and matrix which in turn could exert pronounced effects on creep behavior. Since both the carbide and nitride exhibit solubility in the tantalum alloy matrix, precipitate morphology will be affected by thermal-mechanical treatment.

Since sheet and tubing are the primary end products for which the alloys were being developed, evaluation criteria was based on (1) fabricability, (2) weldability, (3) creep resistance, and (4) liquid alkali metal corrosion resistance. Although the reactive metal additions of hafnium and zirconium would not necessarily make a contribution to the creep strength based on the diffusivity and moduli contribution to the matrix, reactive metal additions were nonetheless needed for liquid alkali metal corrosion resistance.^(15,16)

The commercially available high strength tantalum base alloy T-111 (Ta-8W-2Hf) was used as the base line for property comparison.

B. EXPERIMENTAL PROCEDURES

A detailed description of the procedures and techniques used to prepare, and test the experimental tantalum alloy compositions is found elsewhere.⁽¹⁾ However, the processing and testing techniques will be briefly described. These represent procedures which ensure preparation and processing to final sheet with non-detectable contamination occurring during hot working and intermediate annealing operations.

1. Melting

Experimental alloy compositions were prepared by non-consumable electrode D. C. arc melting ingots weighing 800 grams under a partial pressure of high purity argon or by consumable electrode double vacuum arc melting 2 inch diameter ingots weighing approximately

seven pounds. Starting materials were of the highest purity commercially available and were procured in strip form. Typical analysis of the tantalum and Ta-10W material used for the alloy base is given below in Table 10.

TABLE 10. Analysis of Tantalum and Ta-10W Alloy Base Starting Material

Material	Analysis, ppm									
	C	O	N	Cb	Fe	Si	Mo	Zr	Ti	W
Ta ^(a)	<30	60	25	130	<15	20	10	--	14	585
Ta-10W ^(b)	10	10	10	<500	40	<10	150	--	<10	9.95%

(a) Supplier - Wah Chang

(b) Supplier - Fansteel

Carbon and nitrogen additions to the non-consumable melts were made with +200 mesh TaC and a Ta-1%N alloy respectively. Carbon additions to the consumable electrode melts were made using graphite cloth and nitrated tantalum strips were used to introduce nitrogen. Electrodes for consumable electrode melting were fabricated in sandwich form from strip.

2. Primary and Secondary Working

The as-cast ingot structure was worked by upset forging or extrusion using a Model 1220C Dynapak high energy rate machine. Forging billets were coated with an Al-12Si alloy to provide protection from contamination during heating and to facilitate subsequent conditioning. Extrusion billets were coated with unalloyed molybdenum by plasma spraying to provide oxidation protection during heating and lubrication during extrusion. Extrusion to sheet bar at a 4:1 reduction was done at 2550°F. Heating for forging and extrusion was accomplished by induction under a flowing argon atmosphere. Temperatures were measured using an optical pyrometer.

The as-forged or extruded sheet slabs were examined visually, conditioned, annealed for 1 hour at 3000°F, and then rolled to 0.060 inch sheet (~70% reduction). The 0.060 inch

sheet was then annealed for 1 hour at 3090°F and rolled to 0.040 inch in thickness. All initial breakdown rolling was done at a maximum temperature of 900°F and finish rolling was accomplished at room temperature. All mechanical property tests and weldability evaluations were done on 0.04 inch thick sheet. One hour recrystallization temperature determinations were nominally made on 0.06 inch thick sheet.

3. Welding

Compositions satisfactorily processed to 0.040 inch sheet were welded by both automatic tungsten arc inert gas welding (GTA) and electron beam welding techniques. Automatic tungsten arc inert gas welding was performed in a vacuum purged welding chamber which is continuously monitored for the oxygen and water content in the welding atmosphere⁽¹⁷⁾. All GTA welding was done in a high purity helium atmosphere which contained less than 5 and 1 ppm respectively of oxygen and water vapor. All welds were bead-on-plate with a 100% penetration to simulate butt welding. Parameters used for GTA welding were as follows:

Welding current-100 amps

Welding speed-fifteen inches a minute,

Arc gap-0.06 inches

Clamp spacing-3/8 inch

Electrode diameter-3/32 inch

Electron beam welding was accomplished in a 2 KVA Zeiss Electron Beam Welder. The welding speed was 25 inches per minute with an 0.025 inch traverse deflection of the beam. Welding was done after evacuation of the chamber to less than 5×10^{-6} torr.

4. Mechanical Property Testing

a. Bend Test. The ductile-brittle transition behavior in bending was determined on base metal and on as-GTA and EB welded specimens. Bend test specimens were nominally

1/2 inch wide x 1 inch long x 0.04 inch thick. Specimens supported on a 0.6 inch wide span were loaded at 1 inch per minute deflection rate using a punch with a nose radius of 0.071 inch (bend factor 1.8t). Test temperatures from -320°F to R.T. were obtained using a cryostat which employed a controlled flow of liquid nitrogen. A small resistance heated furnace around the bend test fixture was used to heat specimens for testing above room temperature. A thermocouple located in the nose of the punch was used for monitoring and controlling specimen temperature. No special surface preparation was used on the bend specimens. The base metal specimens were tested in the as-annealed condition and the welded specimens in the as-welded condition with the top of the weld bead the tension side of the bend and with the weld bead perpendicular to the bend axis. The ductile-brittle transition temperature was defined as the lowest temperature at which a full 90° bend could be made without evidence of brittle failure.

b. Tensile Tests. Tensile tests were conducted on 0.04 inch thick sheet metal specimens having a reduced section of 0.250 inches wide by 1 inch long. The strain rate was 0.05 inch per minute based on machine cross head motion. Elevated temperature tests were conducted at a pressure of 1×10^{-5} torr or less. The gauge length of the test specimens was wrapped with tantalum foil to minimize contamination during the test.

c. Creep Test. All creep testing was conducted in sputter ion pumped ultra-high vacuum creep systems of the type described by Buckman and Hetherington⁽³⁾. The creep specimen had a uniform reduced gauge section of 0.250 inch wide x 1 inch long. Temperature was measured with platinum, platinum/rhodium thermocouples tied to the specimen gauge length. Creep strain was measured optically. Test pressure during all creep testing was 1×10^{-8} torr or less. Test specimens were annealed 1 hour at 3000°F prior to test.

5. Heat Treatment

All in-process and final 1 hour vacuum annealing treatments were conducted at pressures of 1×10^{-5} torr or less. All specimens were wrapped in tantalum foil to provide a barrier to contamination during treatment.

6. Recrystallization Behavior

The 1 hour recrystallization temperature was determined on 0.06 inch thick sheet which had been cold reduced 70%. Progress of recrystallization was followed by optical metallography and change in room temperature hardness.

C. EXPERIMENTAL RESULTS AND DISCUSSION

1. Melting

All of the compositions were satisfactorily consolidated by either melting technique. The excellent recovery of both metallic and the intentional carbon and nitrogen additions are illustrated by the chemical analysis results in Table 11.

TABLE 11 - Typical Chemical Analysis Results for Consumable and Non-Consumable Electrode Melted Ingots

Nominal Composition weight percent	Chemical Analysis, weight percent								
	W	Mo	Re	Hf	Zr	C	N	O	
Non-Consumable Electrode Melted									
Ta-8.2W-1Hf-0.035C	8.0	--	--	1.0	--	0.032	--	--	
Ta-8.6W-0.53Hf-0.02C	8.2	--	--	0.51	--	0.021	--	--	
Ta-7.1W-1.56Re-0.26Zr-0.02N	7.0	--	1.6	--	0.23	--	0.012	--	
Consumable Electrode Melted									
Ta-8W-2Hf-0.05C	Top	7.7	--	--	1.74	--	0.054	0.002	--
	Bottom	7.8	--	--	1.83	--	0.051	0.002	--
Ta-5.7W-0.7Mo-1.56Re-0.75Hf -0.13Zr-0.015C-0.015N	Top	6.4	0.65	1.61	0.76	0.12	0.016	0.013	0.0043
	Bottom	6.2	0.65	1.58	0.80	0.12	0.016	0.015	0.0045

2. Primary Fabrication

The forgeability characteristics of the Ta-W-Hf-C compositions studied are summarized in the data plotted in Figure 19. The limit of satisfactory forgeability was fixed where excessive edge cracking occurred during forging. The low solubility of carbon in tantalum, <100 ppm at 3000°F^(10,18,19,20) results in a hard second phase dispersed in a highly ductile matrix. However as the carbon content is increased, the carbide phase becomes continuous. The carbon level at which the carbide phase becomes continuous decreases as the W+Hf solute level increases. As long as the carbide phase was discontinuous, upset forgeability was satisfactory. However as the carbide phase became continuous, poor forgeability as evidenced by excessive edge cracking was observed. This relation of microstructure to forgeability is illustrated in Figure 20.

Substitution of nitrogen for carbon results in degradation of forgeability as the nitrogen level is increased above 400 ppm. Whereas carbon exhibits a very low solubility in the tantalum alloy matrix and dispersed carbide phases are present when the carbon content is less than 100 ppm, nitrogen has an apparent high solubility and as-cast microstructures of compositions containing up to 800 ppm nitrogen appeared single phase. The potent strengthening caused by the nitrogen is illustrated in the data plotted in Figure 21. This would not be unexpected since unalloyed tantalum has a very high solubility for nitrogen (0.58% at 2400°F and 0.44% at 2200°F).⁽²¹⁾ However if the nitrogen occupied only interstitial sites it would not be expected to contribute to the strength at the forging temperature and thus the marginal forgeability characteristics of the 800 ppm containing alloys were not anticipated. Most of the forgeability evaluation data are for non-consumable electrode melted ingots and due to (1) the poor shape of the as-melted ingot and (2) microstructural and compositional heterogeneity intrinsic with non-consumable melted ingots forgeability characteristics are generally poorer than for identical compositions prepared by the consumable electrode melting process. The level of Zr, Mo and Re additions investigated had no apparent effect on forgeability. From binary data reported,⁽²²⁾ equivalent atom percents of Zr and Mo for Hf and W at the solute levels investigated would be expected to behave similarly. The as-cast hardness data of

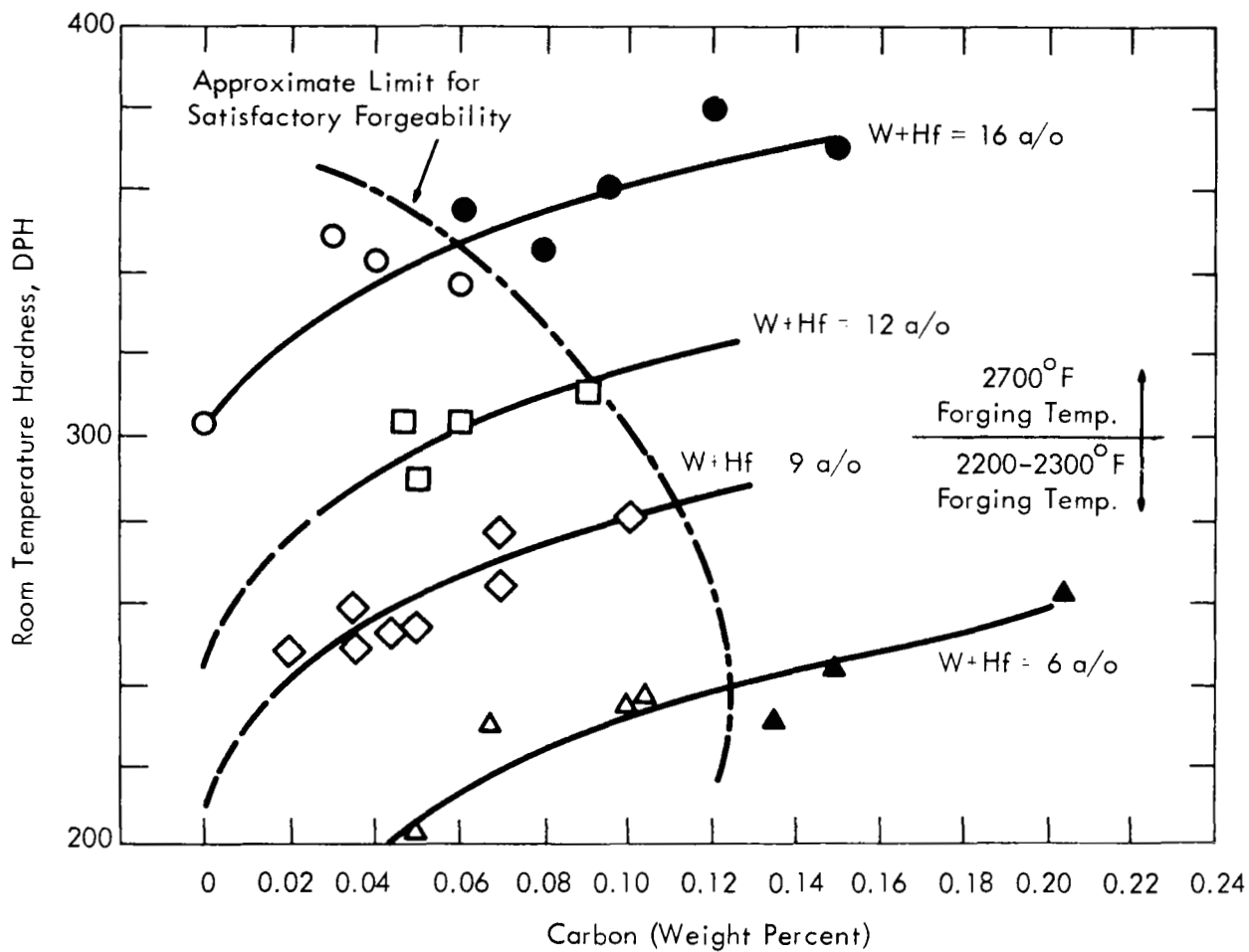
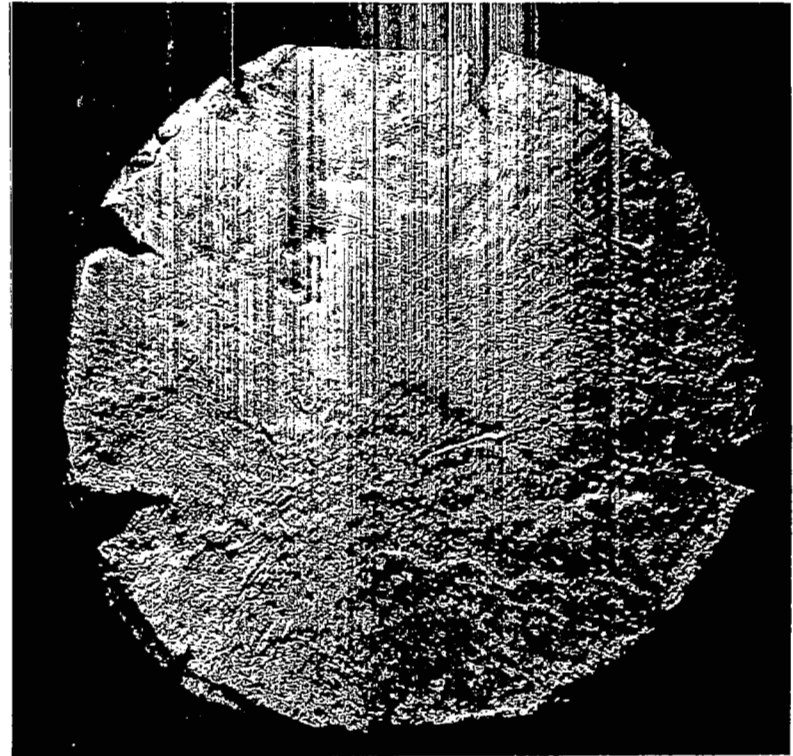
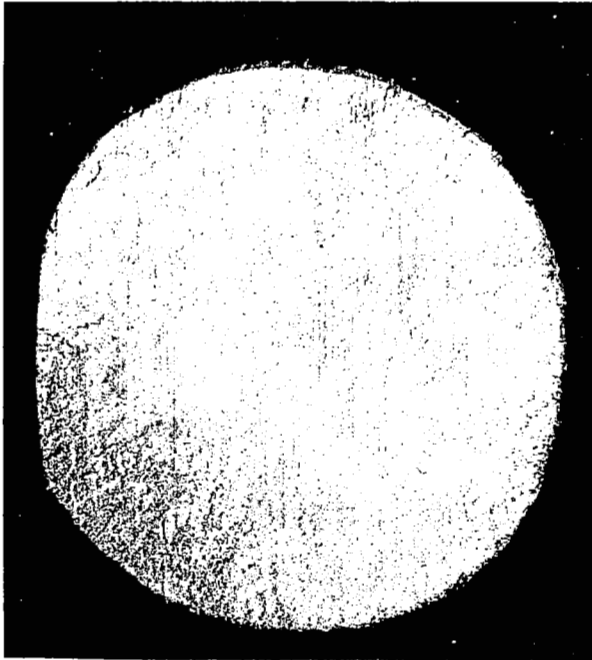
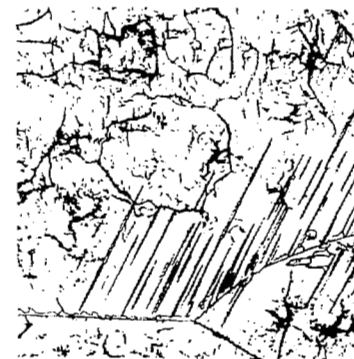


FIGURE 19 - Effect of Carbon on the Forgeability Limit, 50% Upset, of Ta-W-Hf Alloys (Note: Closed Symbols Denote Moderate to Severe Edge Cracking. Open Symbols Denote No or Minor Edge Cracking.)



Ta-8.2W-1Hf-0.07C



Ta-14.6W-1.8Hf-0.12C

FIGURE 20 - As-Forged Button and As-Cast Microstructure

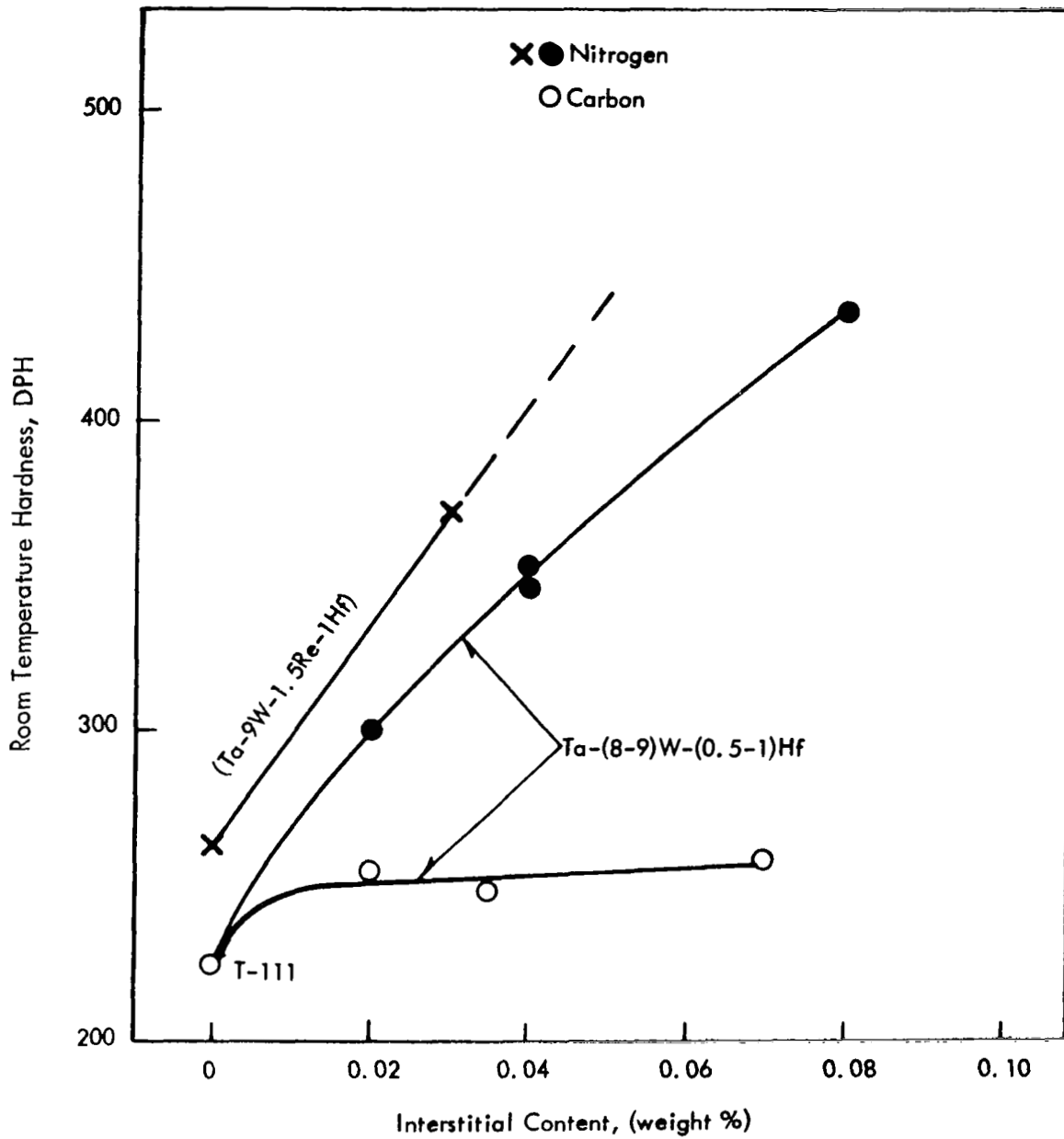


FIGURE 21 - Effect of Carbon and Nitrogen on the Room Temperature Hardness of As-Cast Tantalum Alloys

Figure 21 also indicate that at the Re level studied, its contribution to the room temperature strength is essentially equivalent to that for tungsten. However at rhenium levels $>2a/o$, Re is reported to be about three times more effective in increasing the room temperature yield strength as W.⁽²²⁾

Excellent extrudeability was exhibited by the 2 inch diameter ingot compositions. Extrusion billets after coating with unalloyed molybdenum by plasma spraying were extruded at a 4:1 reduction ratio to sheet bar. A typical as-extruded sheet bar is shown in Figure 22.

3. Secondary Fabrication

The as-forged sheet slabs were conditioned, inspected, annealed for 1 hour at $3000^{\circ}F$ and then rolled to 0.06 inch thick sheet. From the starting thickness to 0.125 inch, the sheet slab was heated to $900^{\circ}F$ for rolling. Rolling from 0.125 inch to 0.06 inch thickness was done at room temperature. This process schedule was selected so that compositions which could be rolled to sheet by this schedule would most likely be readily fabricated to tubing using existing technology.

Generally, the same trends observed for the primary fabricability were applicable to secondary working. Although as expected the lower secondary working temperature resulted in a decrease of fabricability at lower total solute levels. Presented in Figure 23 are the approximate compositional limits within the Ta-W-Hf-C system which produced good quality strip by the previously mentioned rolling schedule. The highly fabricable tantalum base alloy T-111 (Ta-8W-2Hf) was used as the basis for comparison.

The Mo, Re and Zr substitutions for the W and Hf at the solute levels investigated ($W+Hf = 9a/o$) did not significantly alter secondary working characteristics. However, nitrogen had a very deleterious effect on sheet rolling characteristics at levels above 400 ppm. At the 200 ppm nitrogen level, tantalum containing 9-10% W+Hf exhibited excellent secondary working characteristics at room temperature.

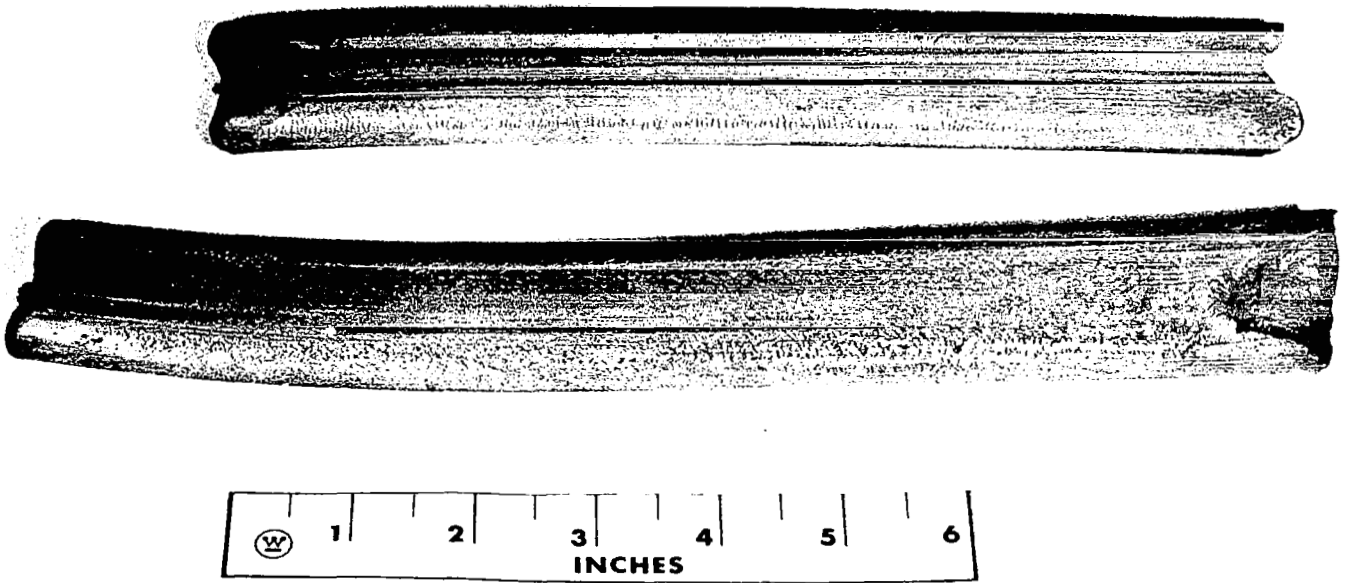


FIGURE 22 - As Dynapak Extruded Tantalum Alloy Sheet Bar

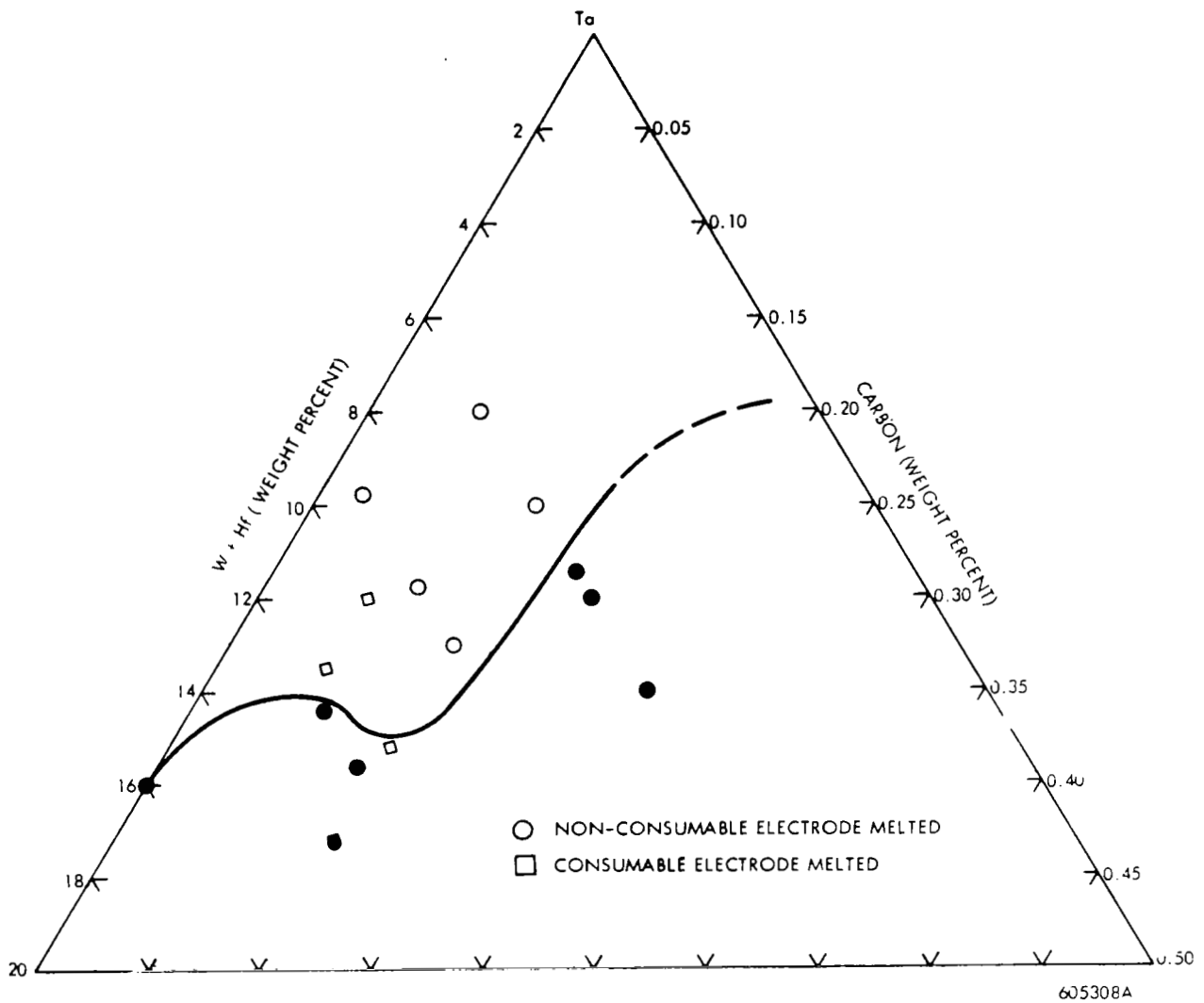


FIGURE 23 - Effect of W, Hf, and C on the Secondary Working Characteristics of Tantalum (Open Symbols Denote Good Quality Strip. Close Symbols Denote Strip Exhibiting Moderate to Severe Edge Cracking.)

4. Fabricability

The primary and secondary working characteristics of the experimental compositions provided a useful screening of compositions which exhibited marginal workability characteristics. However, the change in the bend ductile-brittle transition temperature (DBTT) caused by fusion welding is considered one of the most useful evaluation criterion. The DBTT of as-GTAwelded T-111 is reported as $<-320^{\circ}\text{F}$ ⁽⁹⁾ and the T-111 melted in this investigation behaved similarly. The DBTT for as-GTAwelded Ta-9%(W+Hf) material increased significantly as the carbon content exceeded 200 ppm (see Figure 24) and at 500 ppm carbon, the DBTT was significantly above room temperature. This was a significant increase since the annealed (1 hour at 3000°F (1650°C)) base metal had a DBTT of less than -320°F (-196°C). Transverse sections of the weldments were metallographically examined and single phase fusion and heat affected zones were observed, indicating that during the welding cycle, the heating and cooling rates were sufficient to retain the carbon in solid solution. Hardness traverse data shown in Table 12 confirm that the carbon is indeed in solid solution, and thus the rapid increase in the DBTT temperature should not be unexpected. By an appropriate post weld annealing treatment, the carbon can be precipitated from solid solution resulting in a decrease in the fusion and HAZ hardness and a resultant lowering of the DBTT (see Table 13 and Figure 25). Carbide precipitation from the highly supersaturated solid solution occurred at temperatures as low as 1290°F . Insufficient material did not permit detailed investigation of the lower temperature post weld annealing treatments although annealing for 1 hour at 1470°F resulted in approximately the same room temperature hardness as annealing for 1 hour at 2730°F . However, homogenization and re-distribution of the carbide phase was occurring at the higher post weld annealing temperatures (see Figure 25).

The DBTT of the compositions containing Mo, Zr, Re and N additions was generally higher than for the equivalent Ta-W-Hf-C composition as illustrated by the data plotted in Figure 26 for as-electron beam welded material. The same behavior pattern was observed for the GTA welded material although the rate of degradation was more rapid due in part to the greater volume of cast metal in the GTA weld and the virtual absence of a heat affected zone in the EB weld. At the relatively high interstitial levels, ≥ 400 ppm, separation of individual element effects on weldability is difficult.

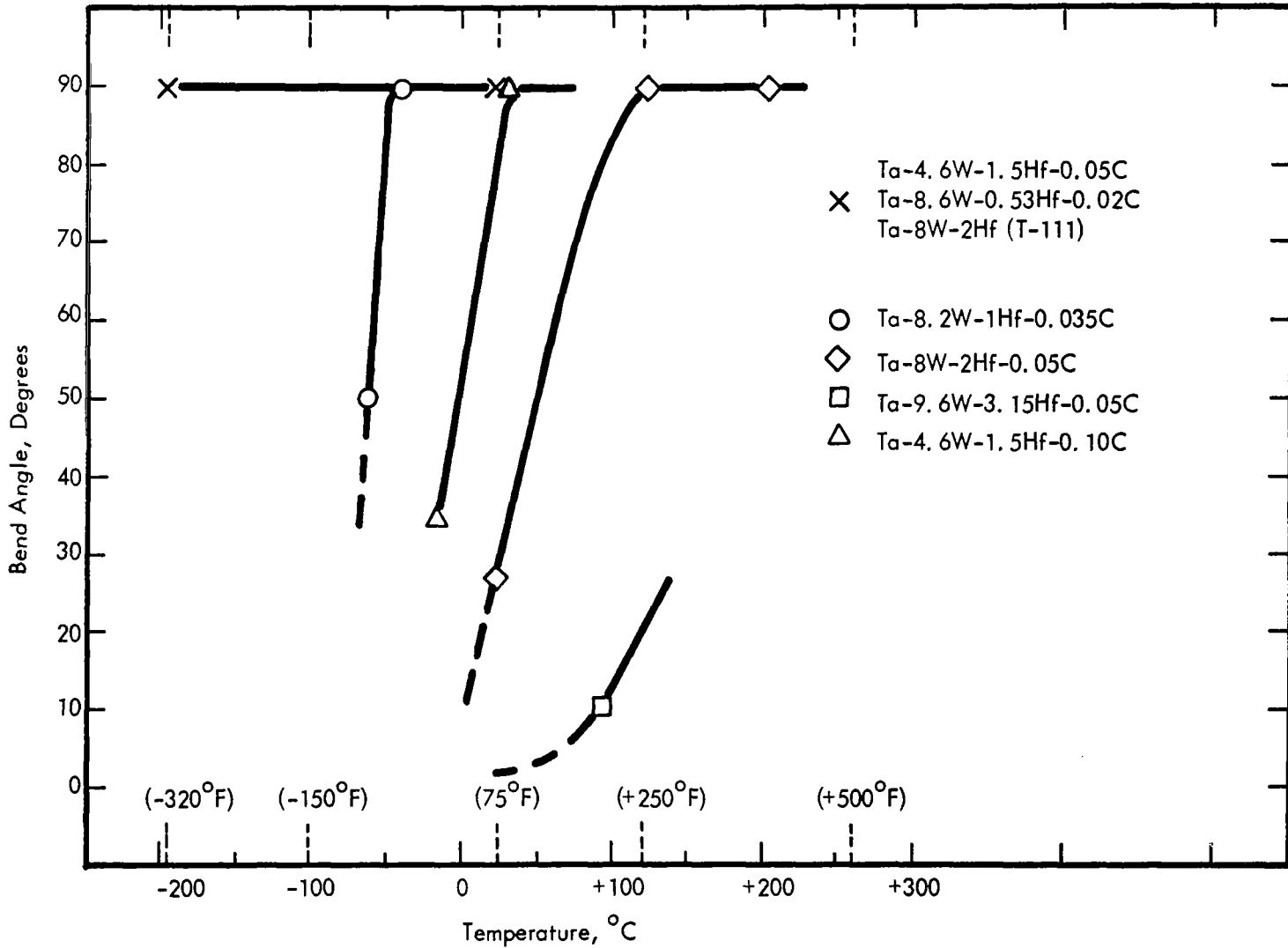


FIGURE 24 - Effect of Carbon on the Bend Ductility of Experimental Tantalum Alloys

TABLE 12 - Hardness Traverse Results for As-GTA Welded Tantalum Base Alloys

Composition	DPH (Kg/mm ²)		
	Fusion Zone	HAZ	Base Metal ^(a)
Ta-8W-2Hf (T-111)	234	236	210
Ta-8.2W-1Hf-0.035C	332	339	250
Ta-8.5W-0.7Hf-0.045C	380	360	250
Ta-8W-2Hf-0.05C	387	388	270
Ta-9.6W-3.15Hf-0.05C	444	416	320

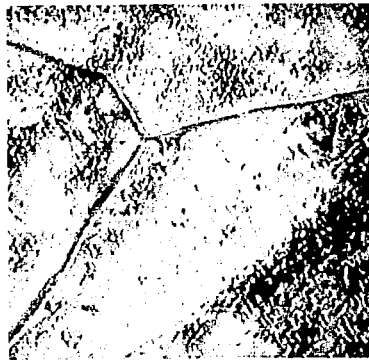
(a) Annealed 1 hour at 3000°F

FIGURE 13 - Effect of 1 Hour Post Weld Annealing on the Fusion and HAZ Hardness of As-GTA Welded Ta-8W-2Hf-0.05C

Location	1 Hour Post Weld Annealing Temperature, °F						
	As-Welded	1290	1470	1830	2010	2550	2730
Fusion Zone	387	305	266	278	277	271	250
HAZ	388	306	262	275	271	268	245



(a) As-GTA Welded
DBTT + 200°F



(b) Post Weld Annealed 1 Hr. at 2550°F
DBTT +75°F



(c) Post Weld Annealed 1 Hr. at 2700°F
DBTT 0°F

FIGURE 25 - Effect of Post Weld Annealing on the Fusion Zone Microstructure and bend DBTT (1.8† Bend Factor) of Ta-8W-2Hf-0.05C (Mag. 1500X)

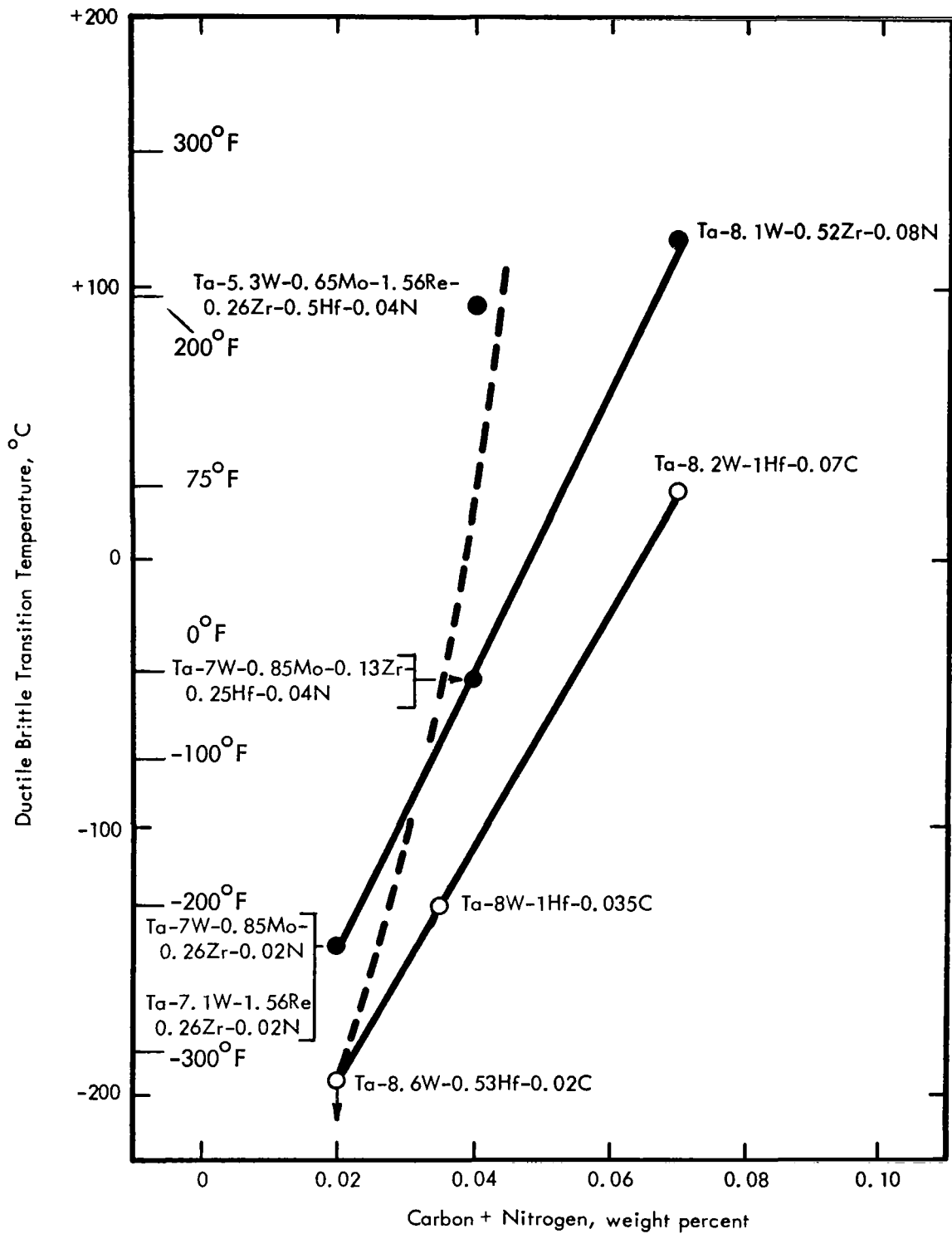


FIGURE 26 - Effect of Carbon and Nitrogen on the Bend Ductile-Brittle Transition Temperature of Experimental Tantalum Alloys

The shift in the ductile-brittle transition temperature caused by welding provides an excellent index to fabricability. Compositions which exhibited a ductile-brittle transition temperature of room temperature and below also had excellent primary and secondary fabrication characteristics. The compositions containing 500-1000 ppm carbon while still exhibiting good fabricability had an as-welded ductile-brittle transition temperature significantly above room temperature. However, good weld ductility can be achieved by a proper post weld annealing treatment (see Figure 25).

5. Recrystallization Behavior

Pure tantalum that has been reduced 75% forms equiaxed grains after heating for 1 hour at 2200°F.⁽²³⁾ The recrystallization temperature for T-111 worked 95% was reported as 2700°F⁽⁹⁾ and the value of 2550°F obtained in this investigation for T-111 (Ta-8W-2Hf) reduced 75% is in good agreement. The addition of carbon to the Ta-W-Hf matrix did not apparently alter recovery but it did effect grain boundary mobility as the hardness minima of the isochronal annealing curves (see Figure 27) did not normally coincide with the complete formation of equiaxed grains. The increase in hardness at the higher annealing temperature is caused by resolutioning of carbon and similar behavior has been reported by other investigators^(8,9,10). Substitution of up to 400 ppm nitrogen did not significantly alter the recrystallization behavior but the high nitrogen bearing composition Ta-5.3W-0.65Mo-1.56Re-0.52Zr-0.08N did not form equiaxed grains until heated at 3630°F for 1 hour. The shape of the isochronal curve for this composition (see Figure 27) suggested the possibility of a precipitation strengthened system. To investigate the response to heat treatment, 0.04 inch thick sheet samples of Ta-5.3W-0.65Mo-1.56Re-0.52Zr-0.08N, Ta-7.1W-1.56Re-0.25Hf-0.13Zr-0.04N, and Ta-8.6W-0.53Hf-0.02C were annealed for 1 hour at 3630°F and rapidly cooled by introducing helium into the furnace chamber. Time for the samples to cool from 3630°F to less than 1470°F was approximately 90 seconds. The as-solution annealed material appeared single phase when examined at 1500X. Specimens of the solution annealed material were then aged for 1 hour at 1290-2400°F and the changes in microstructure were followed by metallographic examination and room temperature hardness measurements (see Figure 28). The

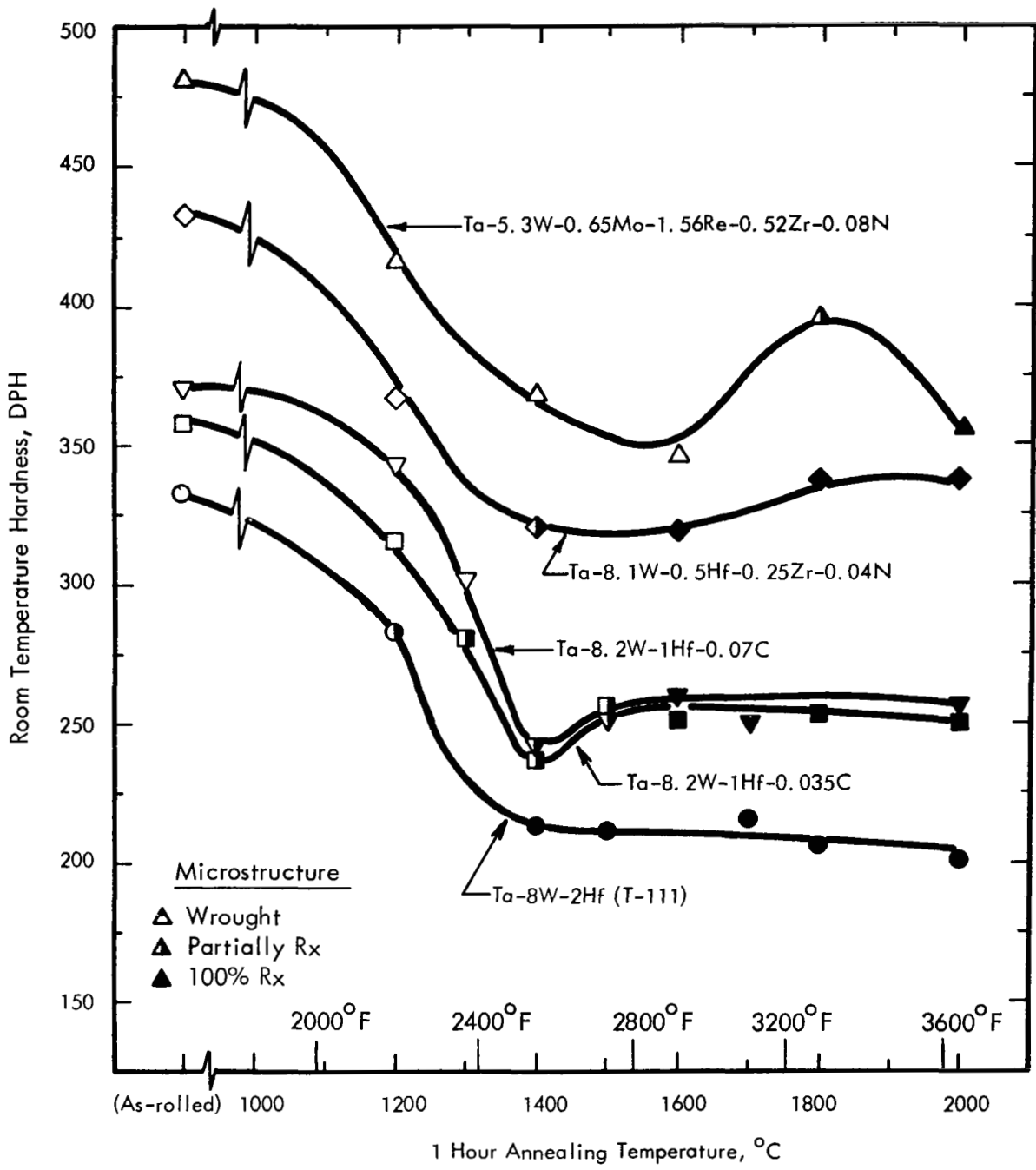


FIGURE 27 - Recrystallization Behavior of Experimental Tantalum Alloy Sheet Given a Prior Cold Reduction of 70-75%

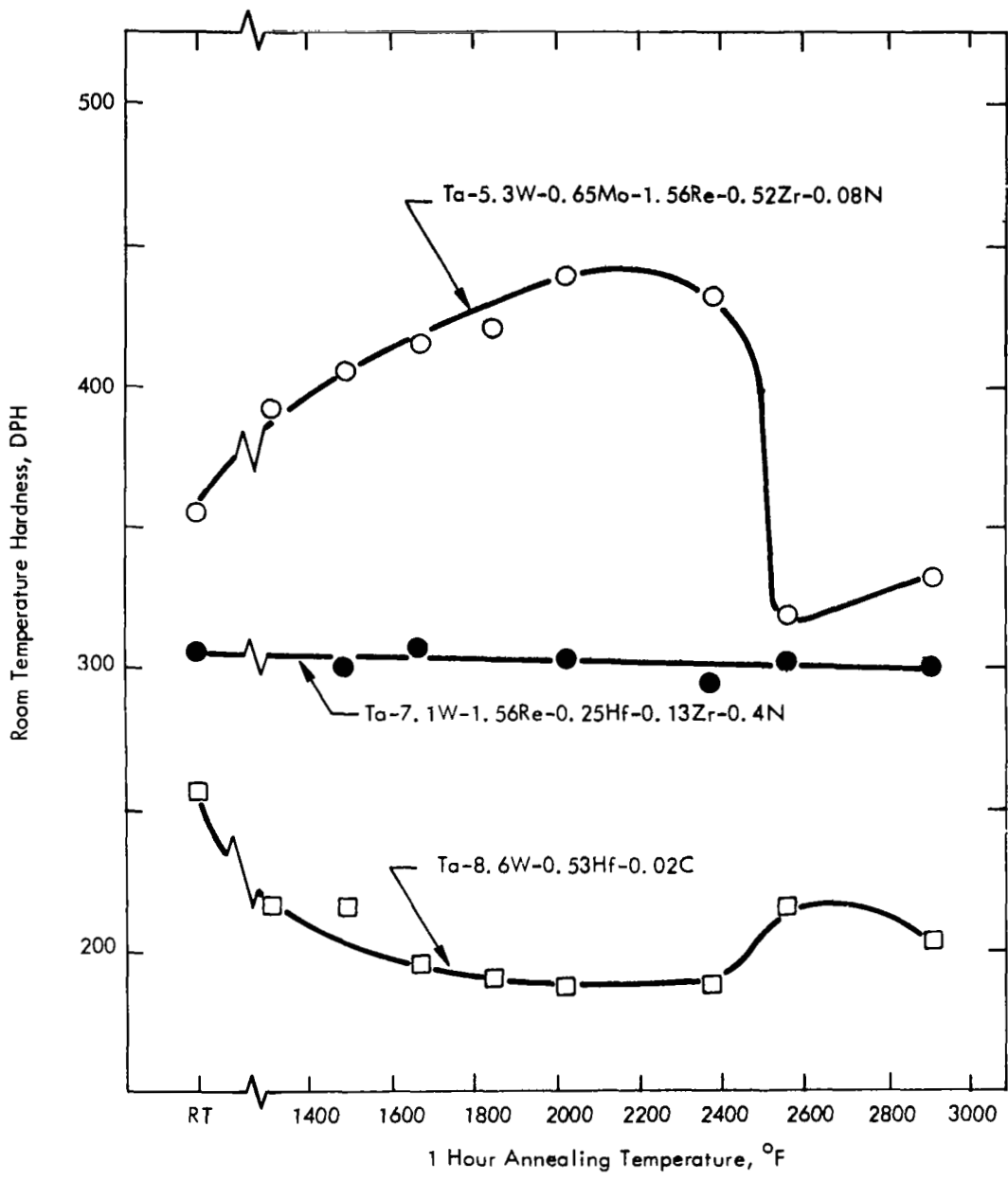
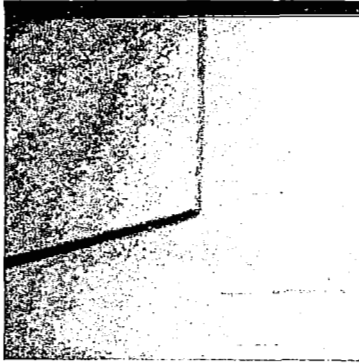
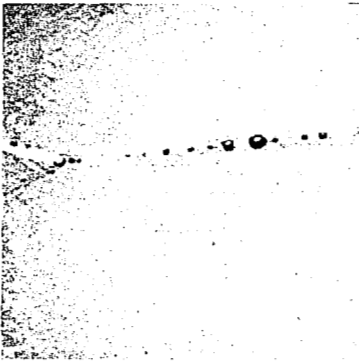


FIGURE 28 - Aging Response of Nitrogen and Carbon Bearing Tantalum Alloys Solution Annealed for 1 Hour at 2000°C and Rapidly Cooled



(a) Aged 1 Hour at 2000°F
360 DPH



(b) Aged 1 Hour at 2370°F
430 DPH



(c) Aged 1 Hour at 2550°F
320 DPH

FIGURE 29 - Microstructure of Ta-5.3W-0.65Mo-1.56Re-0.52Zr-0.08N After Solution Annealing 1 Hour at 3630°F, Rapidly Cooling, and Aging for 1 Hour at the Indicated Temperature. Mag. 1500X

Ta-7.1W-1.56Re-0.25Hf-0.13Zr-0.04N composition did not undergo any change during the 1 hour aging anneals. A single phase microstructure was observed after the 1 hour aging treatments over the entire temperature range investigated. The room temperature hardness of the high nitrogen bearing composition Ta-5.3W-0.65Mo-1.56Re-0.52Zr-0.08N increased after annealing for 1 hour up to 2370°F and then decreased abruptly after 1 hour at 2550°F. Concurrent with this drop in hardness was the appearance of general precipitation throughout the matrix (see Figure 29). No precipitates were observed for samples annealed at less than 2370°F. The sequence of precipitation and change in properties follows coherent precipitation hardening behavior. Similar phenomena has been observed in the Cb-Hf-N system by Begley et al, with overaging occurring at approximately 1830°F.⁽²⁴⁾ The strong evidence for a coherent precipitate is surprising since there is about a 39% misfit between the ZrN and the matrix lattice. Most systems which give to coherent precipitation hardening have misfits between the precipitate and the matrix of only approximately 11%.⁽²⁵⁾

The solution annealed carbon containing composition Ta-8.6W-0.53Hf-0.02C softened on aging at 1290-2370°F indicating the precipitation of a non-coherent precipitate. This behavior was similar to that discussed under the welding section. The dispersed second phases extracted from the Ta-8.6W-0.53Hf-0.02C were identified by x-ray diffraction as the hcp dimetal carbide. The annealing response of GTA welded Ta-9.6W-3.15Hf-0.05C composition which contained only the monometal carbide (Hf,Ta)C_{1-x} exhibited similar behavior.

6. Mechanical Properties

a. Tensile Properties. Generally the addition of carbon to the Ta-W-Hf matrix did not significantly affect room and low temperature ductility although there was an increase in the yield and tensile strength (see Table 14 and Figure 30) as the carbon content and the substitutional solute level was raised. Again substitution of nitrogen resulted in higher room temperature tensile strength due to the potent low temperature strengthening contribution of the interstitial nitrogen as discussed earlier.

TABLE 14 - Room Temperature Tensile Properties of Tantalum Base Alloys Annealed 1 Hour at 3000°F Prior to Test

Composition (w/o)	0.2%Y. S. (psi)	UTS (psi)	% Elongation	
			Uniform	Total
Ta-8W-2Hf (T-111)	69,000	85,900	20.2	36.3
Ta-8W-2Hf-0.05C	74,600	105,000	15.6	21.8
Ta-8W-3.15Hf-0.1C	98,100	126,300	16.2	28.0
Ta-9.6W-3.15Hf-0.05C	107,900	129,500	18.6	28.7
Ta-8.2W-1Hf-0.035C	71,400	102,000	18.3	29.7
Ta-11.3W-0.92Hf-0.06C	101,800	126,200	14.7	22.3
Ta-9W-1Hf-0.025C	78,600	106,800	14.8	23.5
Ta-8W-1Re-0.7Hf-0.025C	78,000	105,000	16.7	28.0
Ta-7W-0.85Mo-0.025Hf-0.13Zr-0.04N	121,200	130,800	14.2	20.3
Ta-7W-0.85Mo-0.26Zr-0.02N	101,000	111,700	15.6	25.6
Ta-5.7W-0.7Mo-1.56Re-0.25Hf-0.13Zr-0.017C-0.02N	127,100	134,000	13.0	23.8
Ta-7.1W-1.56Re-0.26Zr-0.02N	106,600	118,500	15.6	25.9
Ta-8.7W-0.26Zr-0.008C-0.01N	99,800	113,200	14.2	22.0
Ta-7.5W-1.5Re-0.54Hf-0.015N-0.015C	132,200	138,800	8.6	15.3
Ta-6.5W-2.5Re-0.3Hf-0.01C-0.01N	142,000	146,300	6.5	12.7
Ta-4W-1Mo-2Re-0.3Zr-0.015C-0.015N	138,200	142,700	10.4	17.3
Ta-9.5W-0.5Re-0.25Zr-0.02C-0.01N	102,000	116,400	15.9	28.9
Ta-4W-3Re-0.75Hf-0.01C-0.02N	132,000	133,200	12.2	22.7
Ta-5W-1Re-0.3Zr-0.025N	110,300	112,300	11.6	18.5

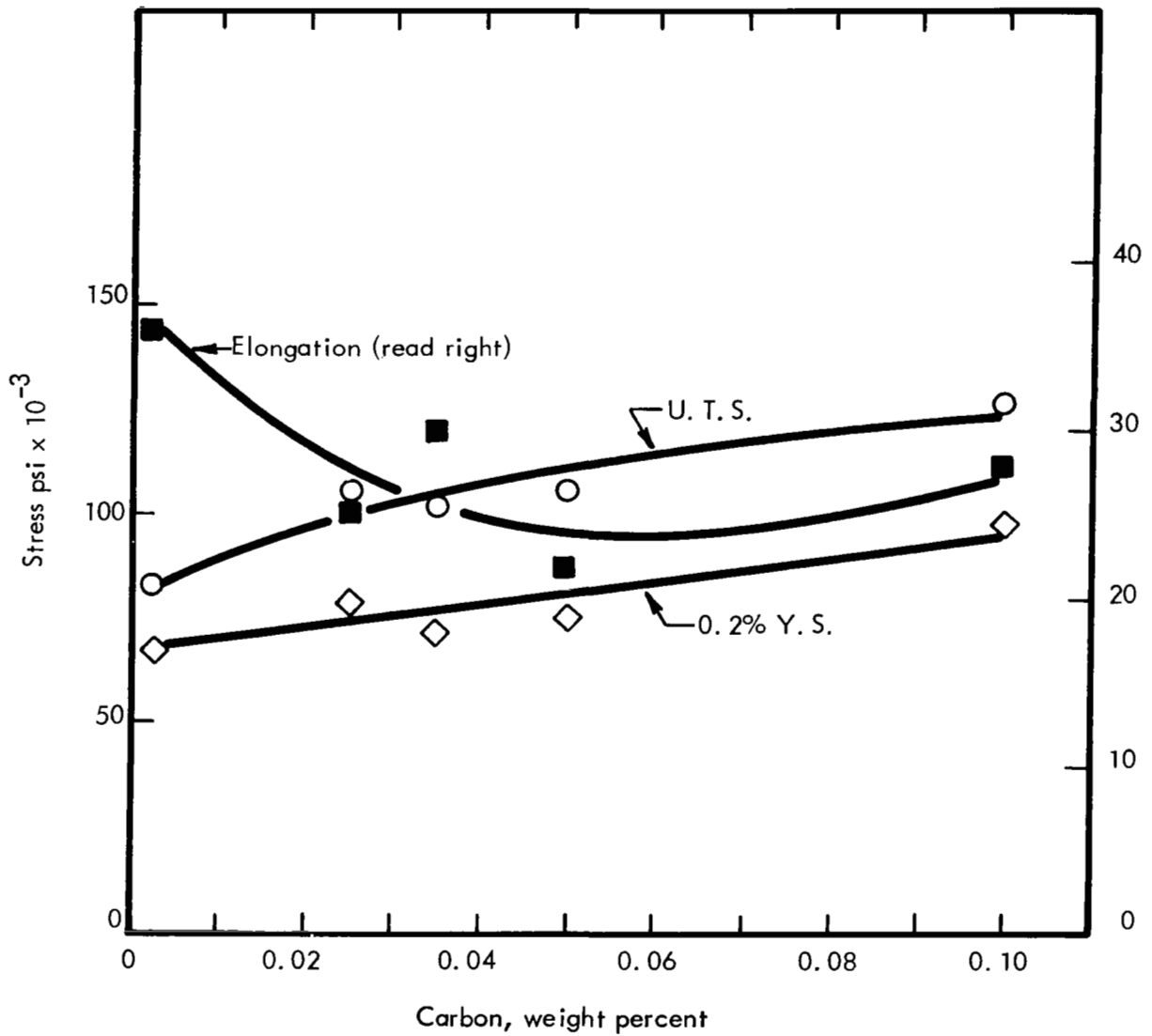


FIGURE 30 - Effect of Carbon on the Room Temperature Tensile Properties of Ta(8-9)W-(1-3)Hf Alloys (Annealed 1 Hour at 3000°F (1650°C) Prior to Test)

Carbon additions significantly increase the yield strength at 2400°F and appears to be effective even at 3000°F although to a much lesser extent (see Table 15 and Figure 31). The short time strength improvement is no doubt related to a dispersed phase strengthening mechanism as it would be unlikely that interstitial carbon would effect mechanical properties at this temperature. Substitution of nitrogen for carbon results in an additional increase in the yield strength at 2400°F but had no effect at 3000°F. The potent short time strengthening of the nitrogen is illustrated by the data in Table 16. The 105,000psi ultimate strength at 2400°F of composition Ta-5.6W-0.65Mo-1.56Re-0.52Zr-0.08N is truly remarkable considering that it contains only 9% substitutional solute. This composition tested at room temperature after annealing for 1 hour at 3000°F exhibited a 141,000 psi yield strength with 13.7% uniform elongation and a total elongation of 17.6%. The annealing treatment did not recrystallize the specimen but resulted only in a stress relief as the recrystallization temperature for this composition was 3630°F as discussed earlier.

b. Creep Properties. Although short time tensile properties were determined to better characterize the strength level and to assess the effects of the solute additions, resistance to creep deformation was the mechanical property of prime interest in this investigation. Initial screening tests were conducted at 2400°F and at stress levels ranging from 10,000 to 20,000 psi. All specimens were annealed for 1 hour at 3000°F prior to test. However creep behavior is a very structure sensitive property and it was not feasible to standardize on the final metallurgical condition. Thus observations on the effects of the various solute additions are qualitative realizing that the structure contributions could not be separated because of the wide composition range studied. The shape of the creep curves that were obtained at 2400°F were characteristically identified by essentially no elongation on loading, an incubation period during which little or no extension occurs and then extension at a constantly increasing rate (see Figure 32). Therefore the time to elongate 1% was the creep evaluation criteria used since the nominally used value of ($\dot{\epsilon}_s$) secondary creep had little significance. This characteristically shaped creep curve has been observed by other investigators

TABLE 15 - Elevated Temperature Tensile Properties of Experimental Tantalum Alloy Sheet (Annealed 1 Hr. at 3000°F Prior to Test)

Composition (w/o)	Test Temperature (°F)	0.2% Offset Y. S. (psi)	UTS (psi)	Elongation (%)
Ta-8W-2Hf (T-111)	2000	28,000	52,900	24
	2400	23,400	36,400	40
	3000	18,000	19,500	36
Ta-8W-2Hf-0.05C	2400	33,700	47,400	36
	3000	22,500	24,400	95
Ta-8W-3.15Hf-0.01C	2400	37,800	51,500	38
	3000	24,700	25,700	135
Ta-9W-1Hf-0.025C	2000	33,400	72,800	21
	2400	29,400	43,200	36
	3000	19,400	20,600	71
Ta-7.5W-1.5Re-0.5Hf -0.015C-0.015N	2400	32,200	44,900	29
	2800	25,400	28,900	50
Ta-6.5W-2.5Re-0.3Hf -0.01C-0.01N	2400	32,300	42,800	38
	2800	22,900	26,000	42
Ta-4W-1Mo-2Re-0.3Zr -0.015C-0.015N	2400	37,000	51,500	28
	2800	23,000	25,400	31
Ta-9.5W-0.5Re-0.25Zr -0.02C-0.01N	2400	34,100	47,700	24
	2800	29,800	33,100	24
Ta-4W-3Re-0.75Hf-0.01C -0.02N	2400	34,800	45,600	29
	2800	25,400	27,600	50
Ta-5W-1Re-0.3Zr-0.025N	2400	25,700	39,700	26
	2800	20,800	22,700	46
Ta-5.7W-1.56Re-0.7Mo -0.25Hf-0.13Zr-0.015C -0.015N	2000	41,200	69,800	22
	2400	36,300	48,900	29
	3000	21,800	22,700	64
Ta-8.5W-1.5Re-1Hf	2400	24,900	35,900	19
	2600	24,500	32,000	21
	3000	22,000	23,500	11
Ta-10W-1Re-0.5Hf	2400	23,400	34,300	27
	2600	23,000	30,000	27
	3000	20,500	22,100	18

TABLE 16 - Effect of Nitrogen on the 2400°F Tensile Strength
of Tantalum Alloys Tested in the As-Worked Condition
(Prior 33% Reduction)

Composition	Yield Strength (psi)	Tensile Strength (psi)
Ta-7.1W-1.56Re-0.26Zr-0.02N	61,300	67,900
Ta-5.3W-0.65Mo-1.56Re-0.52Zr -0.08N	80,800	105,100

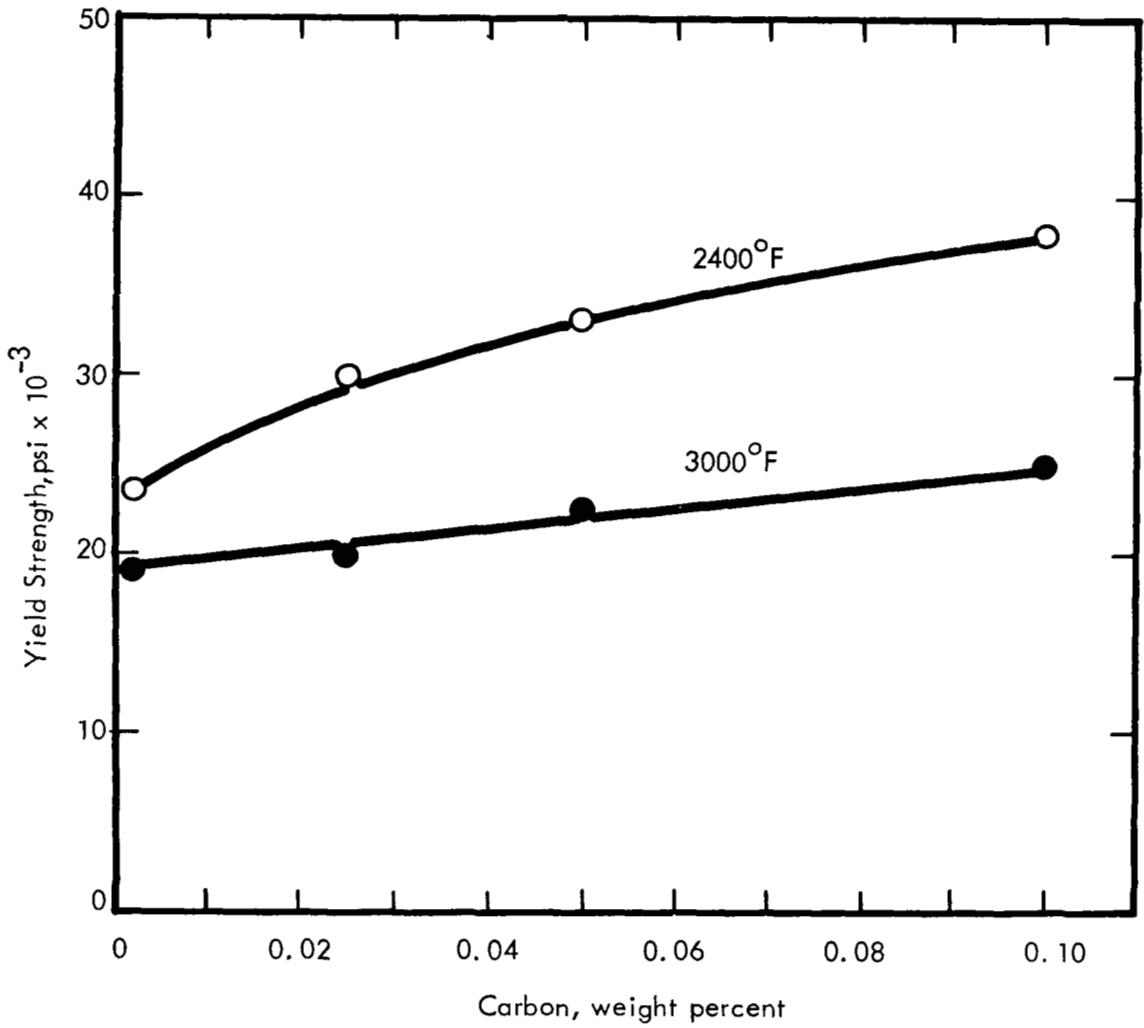


FIGURE 31 - Effect of Carbon on the Elevated Temperature Tensile Strength of Ta-(8-9)W-(1-3)Hf Alloys (Annealed 1 Hour at 3000°F (1650°C) Prior to Test)

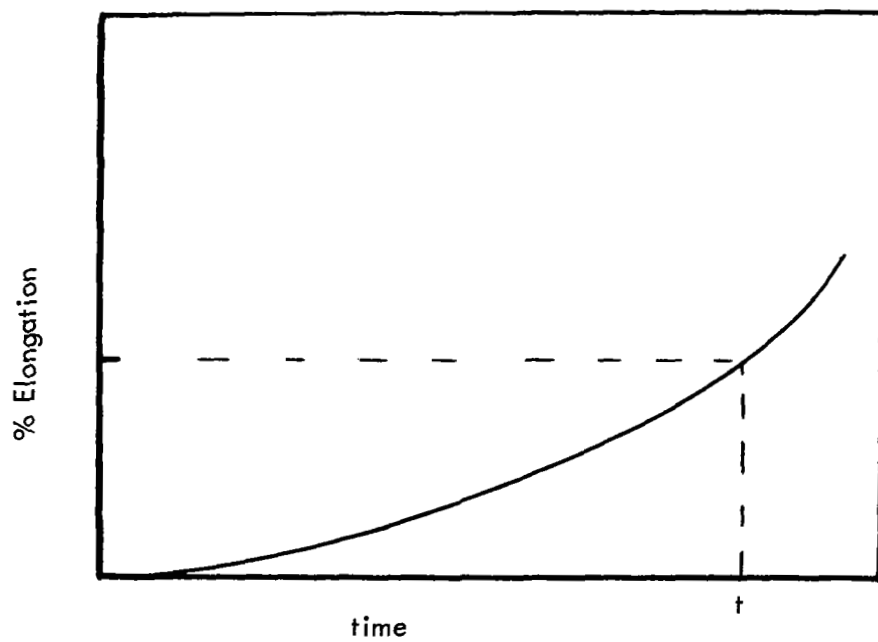


FIGURE 32 - Typical Creep Curve Shape at 2400°F (1315°C) Obtained in Deadweight Loaded Ultra-High Vacuum Creep System

who have tested tantalum and columbium base alloys in deadweight loaded systems under ultra-high vacuum conditions.^(4,26,27)

Carbon additions to the Ta-W-Hf matrix result in an improvement in creep resistance, indicating that the dispersed carbide phase is making a significant contribution to creep resistance (see Figure 33). However, it is also apparent from Figure 33 that for the conditions of test, there is a maximum carbon content (300 ppm) above which the creep resistance is degraded. Thus it would appear that there is an optimum carbon content for creep resistance. Although not confirmed metallographically, it is postulated that since all specimens were given the same final annealing treatment, the resulting carbide phase was much coarser in the higher carbon containing alloys. The carbon solubility in the Ta-W-Hf matrix at 3000^oF is approximately 100 ppm, thus only a small fraction of the carbon of the high carbon containing alloys was dissolved at the final annealing temperature of 3000^oF. It would be expected that if the solvus was exceeded and the cooling sufficient to precipitate a fine carbide phase that the creep resistance would naturally be higher for the higher carbon containing compositions. However, the Ta-W-Hf matrix containing 9-10%W+Hf could withstand only about 300 ppm carbon before as GTA welded bend ductility was seriously degraded. Thus there was little practical interest in further investigation of the higher carbon containing compositions.

Carbide precipitates extracted from the tested creep specimens were identified as either or mixtures of the dimetal and monometal carbide phases. The 2400^oF creep behavior of the experimental Ta-W-Hf-C alloys is summarized in Figure 34. Illustrated here is the time-elongation history curves which could be separated, based on the precipitating phase. It is apparent from Figure 34 that the compositions exhibiting the best creep resistance contained only the dimetal carbide (Ta₂C) as the precipitating phase while the compositions containing only the monometal carbide (TaHf)C_{1-x} exhibited the poorest creep resistance.

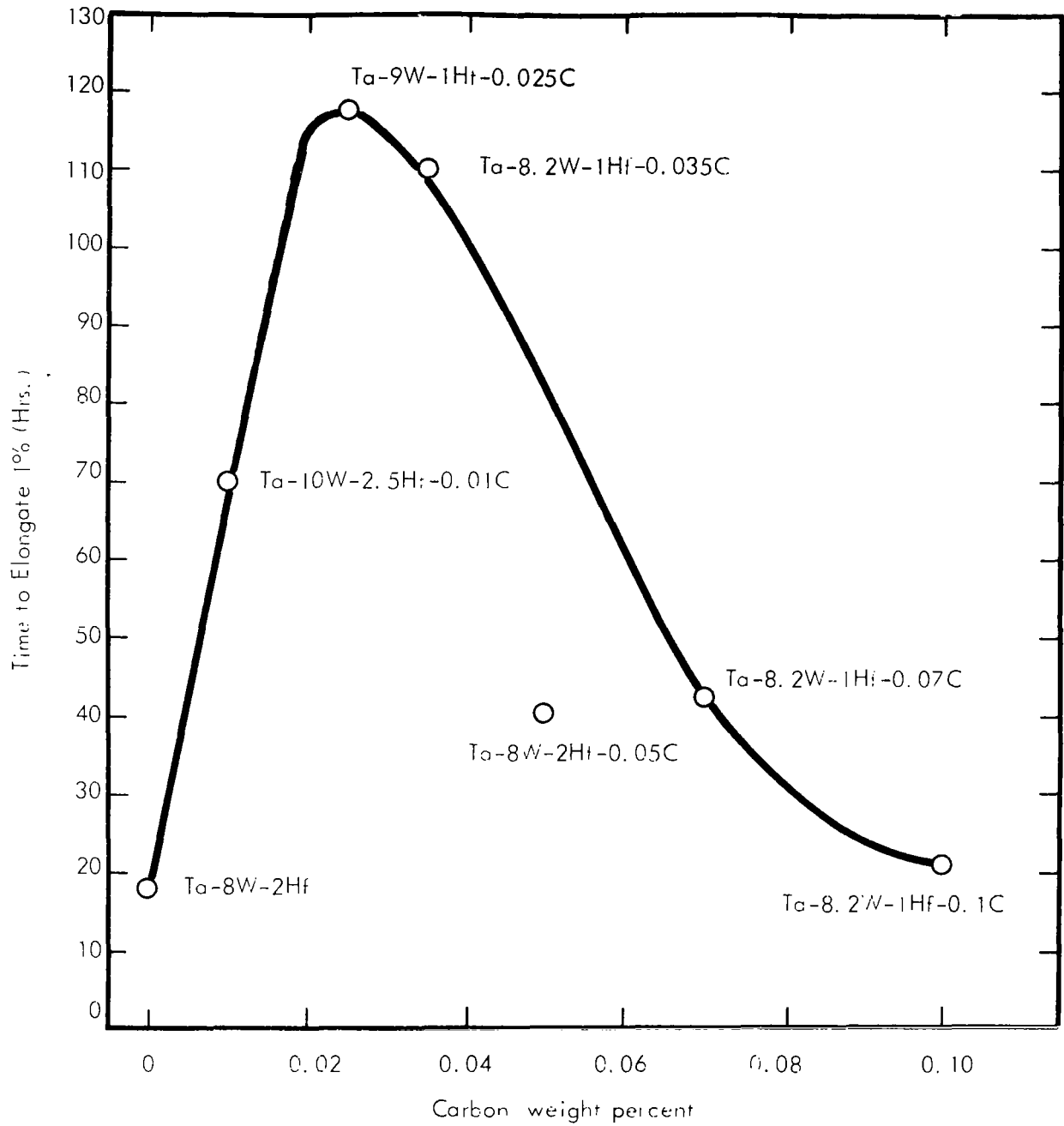


FIGURE 33 - Effect of Carbon on the Creep Behavior of Ta-W-Hf Alloys at 2400°F (1315°C) and 15,000 psi (Annealed 1 Hour at 3000°F (1600°F) Prior to Test)

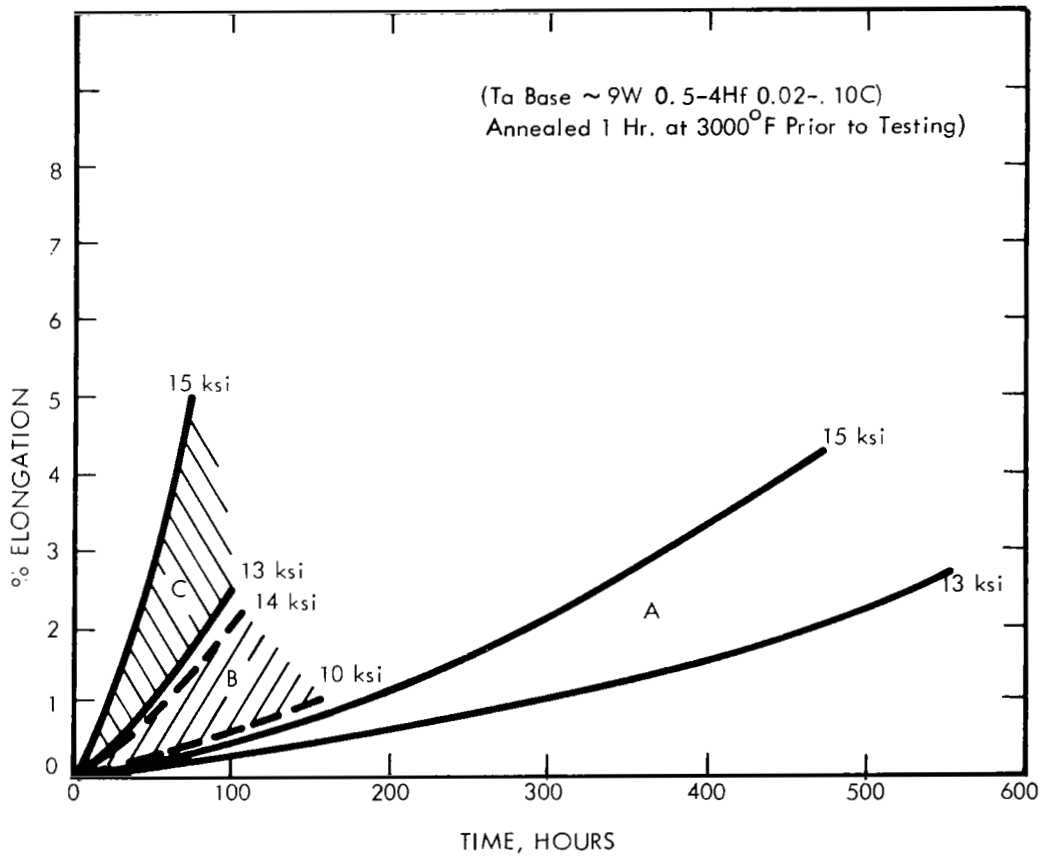
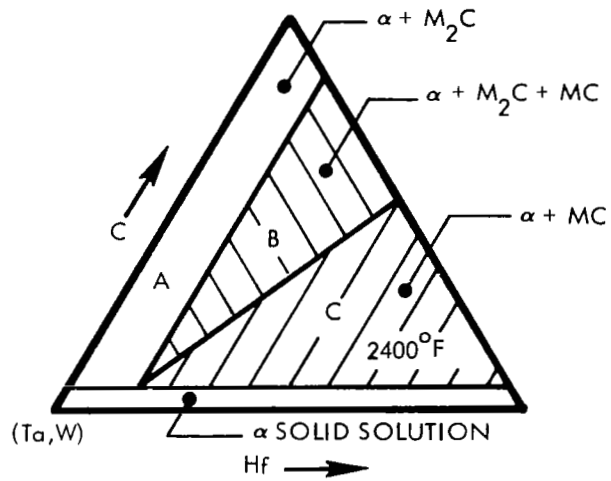


FIGURE 34 - 2400°F Creep Behavior of Ta-W-Hf-C Alloys

During the investigations of Cb-W-Zr-C alloys, it was reported that optimum creep resistance was achieved when the reactive metal/carbon ratio approached unity and here the precipitating phase was identified as the monometal carbide.⁽²⁸⁾ The work on the columbium alloys preceded development of similar tantalum alloys and it was assumed that the same phase relationships would exist at similar composition levels. Thus it would appear that it is not the composition of the carbide phase that is critical, but it is the morphology and distribution which are contributing to the observed creep behavior. At the 500 ppm carbon level for example, reactive metal additions of approximately 3% were required to stabilize the monometal carbide phase. Thus there is always an excess of reactive metal which is present as a substitutional solute. From theoretical considerations, it would be predicted that a reactive metal added for substitutional solute strengthening would result in degradation of creep resistance.^(1,13,14) This behavior is illustrated in Figure 35 as the reactive metal addition exceeds one atom percent. Thus it is futile to attempt to stabilize the monocarbide phase since the reactive metal addition causes a precipitous decrease in creep resistance. Although there was a decrease in creep resistance as the reactive metal content was increased, the elevated temperature tensile strength increased which illustrates the fallacy of extrapolating long time behavior from short time property data.

The minor compositional variations investigated by substituting different atom species, i.e., nitrogen for carbon and rhenium and molybdenum for tungsten provided a dramatic change in the 2400°F (1315°C) creep resistance. As shown in Figures 36 and 37 the tantalum compositions with a nitride dispersion exhibit better creep resistance than those containing the carbide dispersion. The creep curves b, c, d and e in Figures 36 and 37 are for tantalum alloys having 9 atom percent substitutional solute additions ($W+Mo+Re+Hf+Zr = 9 \text{ a/o}$) and have a carbon + nitrogen/hafnium + zirconium atom ratio of 0.5. The carbon precipitates as Ta_2C and involves none of the reactive metal additions. However, the nitrogen precipitates as the reactive metal mononitride, thus effectively removing the Hf and/or Zr from solid solution. As the volume fraction of nitride was increased, a further improvement in creep resistance was observed (see Figure 37, curves e and f). The remarkable strength properties of

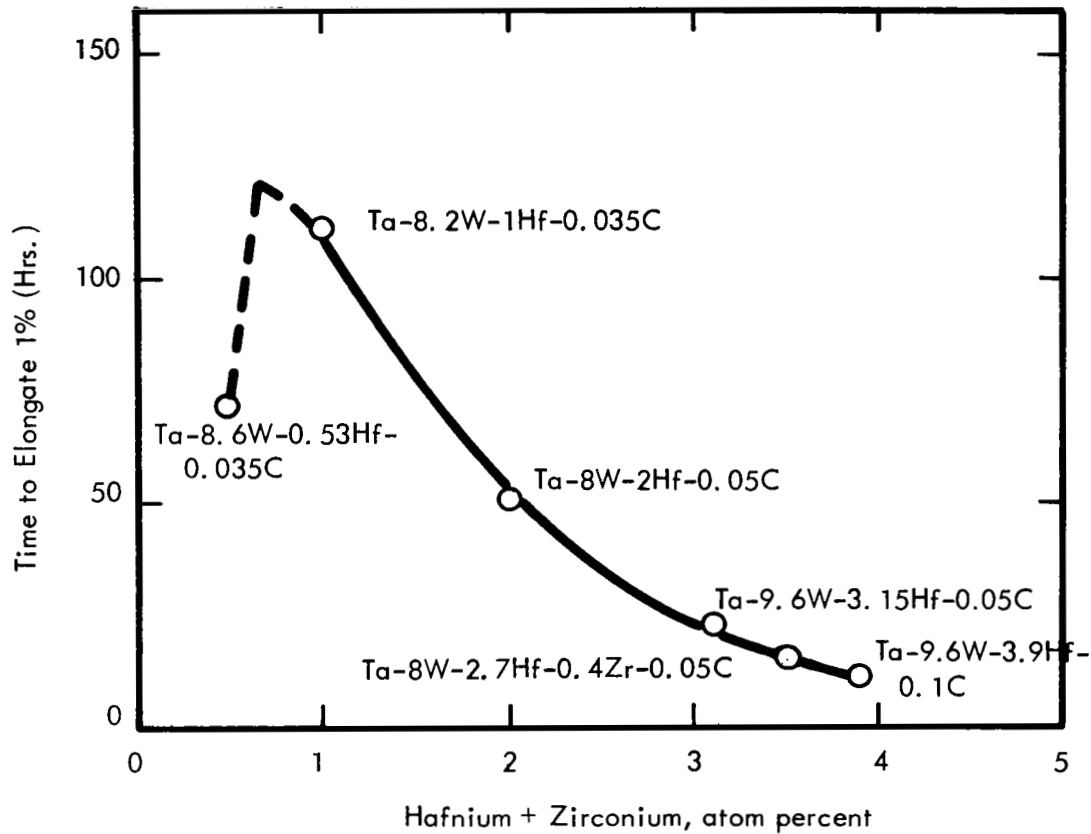


FIGURE 35 - Effect of Reactive Metal (Hf+Zr) Addition on the Creep Behavior of Tantalum Alloys Tested at 2400°F and 15,000 psi

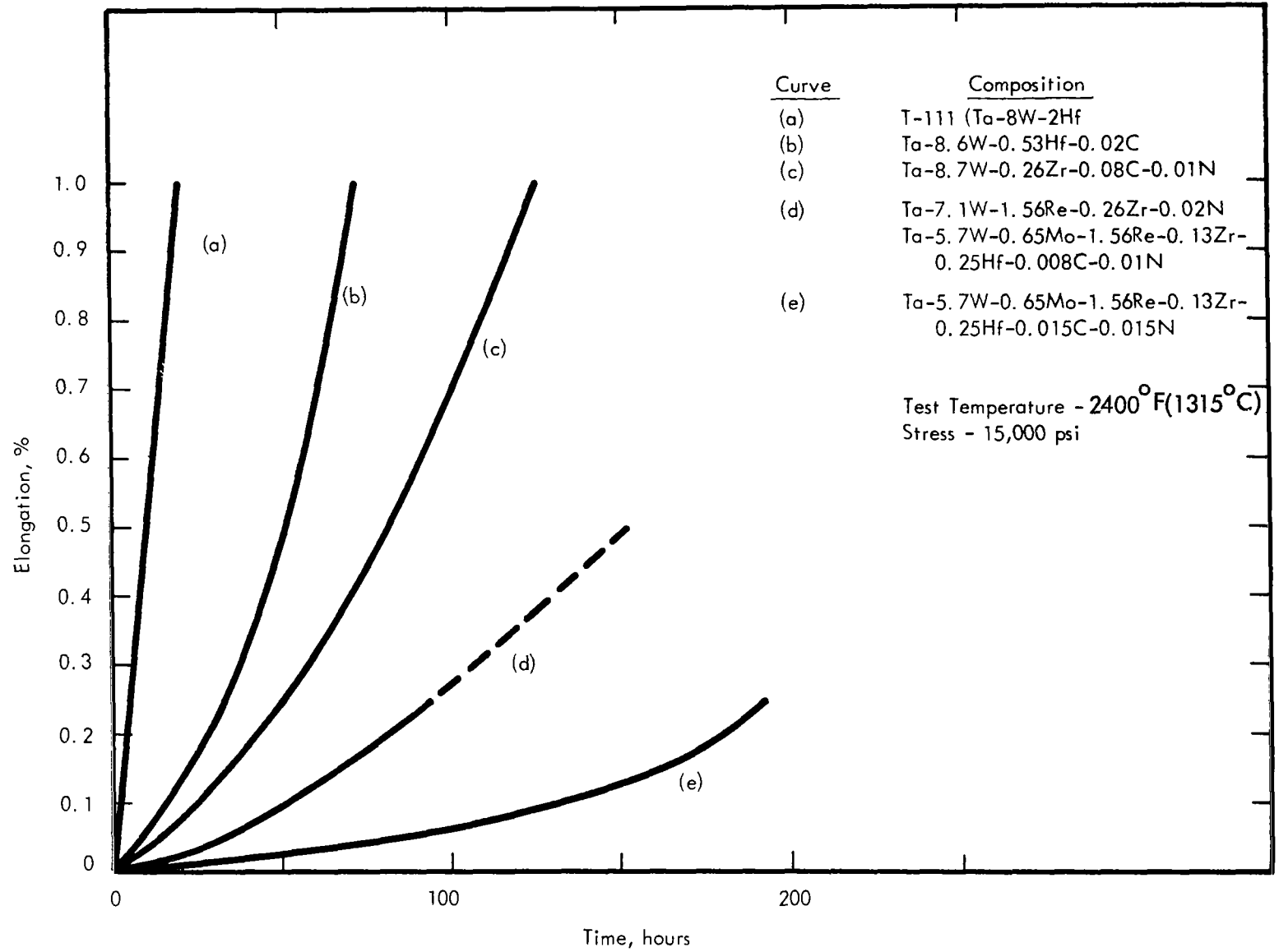


FIGURE 36 - Effect of Composition on the Creep Behavior of Experimental Tantalum Alloys

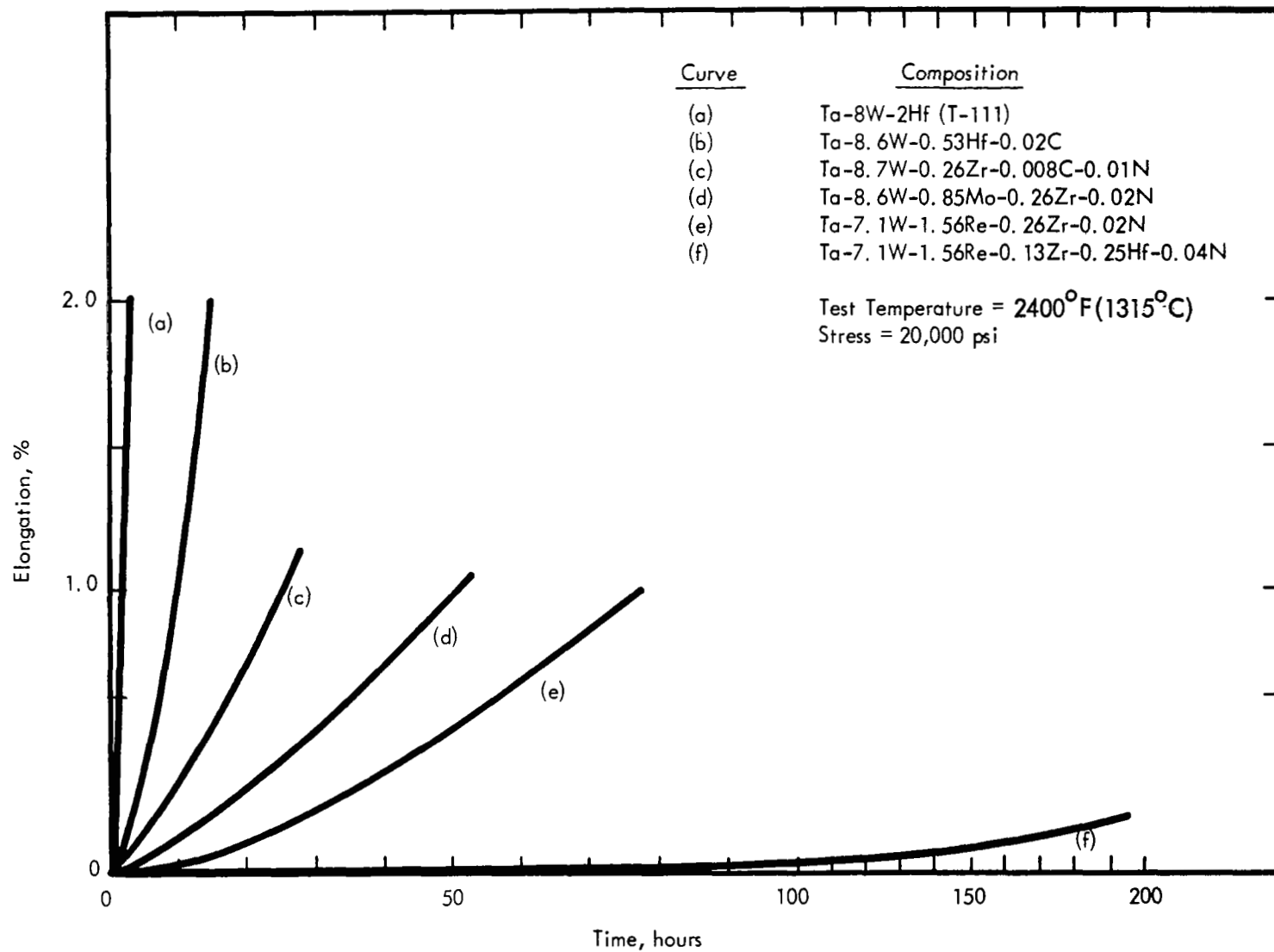


FIGURE 37 - Effect of Composition on the Creep Behavior of Experimental Tantalum Alloys

the nitride bearing compositions is evidenced by the composition Ta-5.3W-0.65Mo-1.56Re-0.52Zr-0.08N. In the as-worked 33% prior reduction, the ultimate tensile strength at 2400°F was 105,000 psi and the 0.2% offset yield strength was 80,000 psi. When given a prior anneal of 1 hour at 3000°F which results in overaging, and then tested in creep at 2400°F and 20,000 psi, the specimen elongated 1% in 124 hours. Although this composition demonstrated remarkable strength properties, the fabricability and weldability characteristics were such that it could not be considered a sheet alloy but it does possess considerable potential as a bar and forging alloy.

Of the substitutional solute additions, the effect of rhenium additions on creep strength was most interesting. Rhenium additions do not significantly improve the short time tensile properties of tantalum until added at the 3% level. However, at this level, a significant degradation of the as GTA welded bend ductility occurs. However, minor amounts of rhenium exert a pronounced influence on creep behavior as illustrated in Figure 38. For example at the 1% level, rhenium exerts a pronounced effect on creep properties but has not altered tensile properties or low temperature ductility as illustrated by the data in Table 17.

A fairly wide range of creep behavior was exhibited by the experimental tantalum alloy compositions investigated. The range of properties obtained which represent a significant improvement over the properties exhibited by T-111 are compared in Figure 39 on a parametric plot. The stress for time to 1% elongation is normalized using the Larson-Miller relation $P = T_o R (\text{constant} + t)$ where t is the time in hours to elongate 1%. Also on the same figure is data for a high strength, highly fabricable columbium alloy Cb-27Ta-10W-1Zr (FS-85).

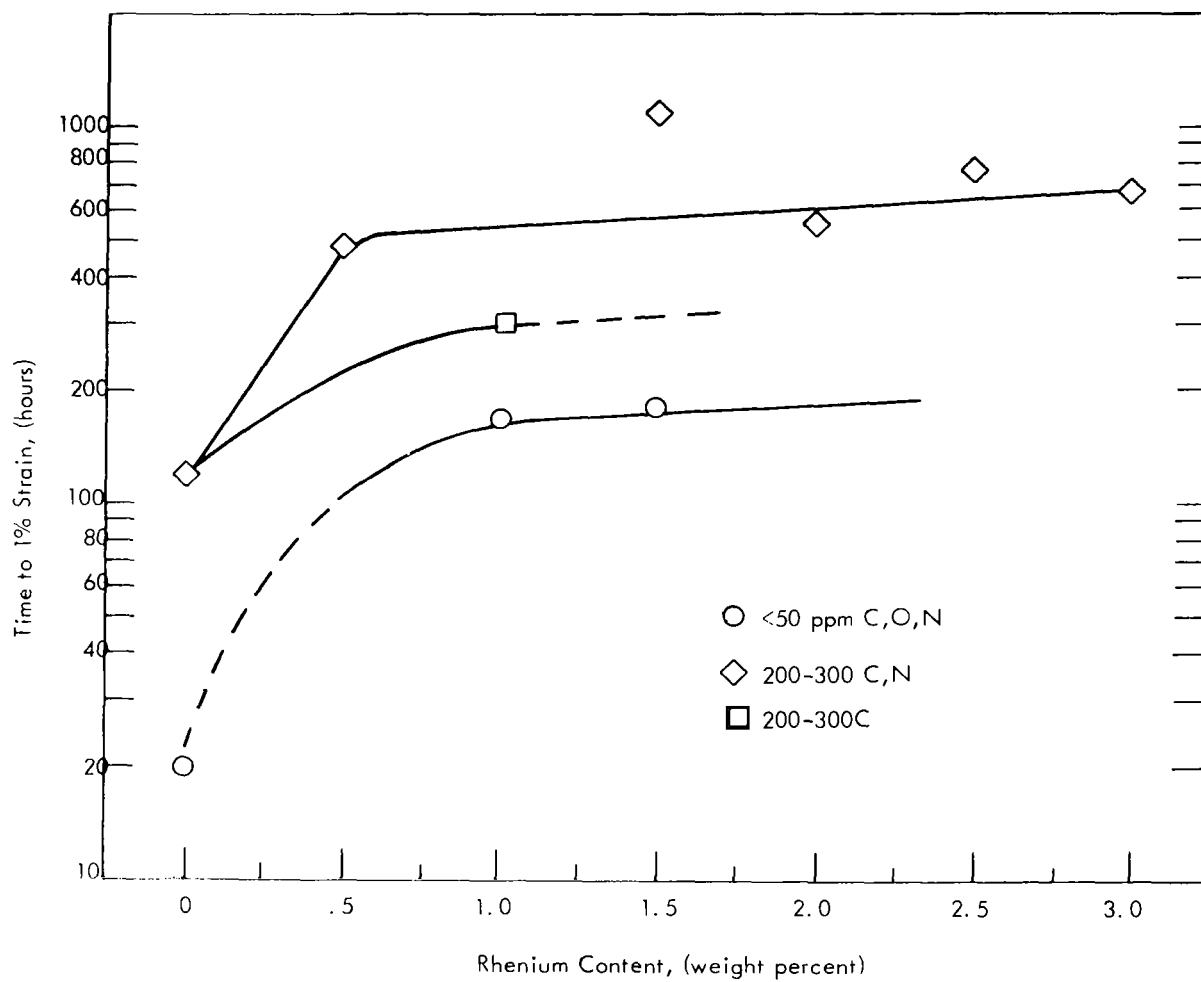


FIGURE 38 - Effect of Rhenium on the Creep Behavior of Tantalum Alloys

TABLE 17 - Effect of Rhenium on Properties of Ta-W-Hf-C Alloy

Property	Composition, w/o	
	Ta-9W-1Hf-0.025C	Ta-8W-1Re-0.7Hf-0.025C
Room Temperature		
Tensile Strength	106,800 psi	105,400 psi
0.2% Yield Strength	78,600 psi	85,000 psi
% Elongation	24%	26%
2400°F		
Tensile Strength	43,200 psi	40,900 psi
0.2% Yield Strength	29,400 psi	30,400 psi
% Elongation	36%	35%
Creep Strength		
Time to 1% elongation at 2400°F & 15,000 psi	108	260
Bend Ductile Brittle Transition over 1t Bend Radius		
Base Metal	<-320°F	<-320°F
As-TIG Welded	-150°F	-150 to -250°F

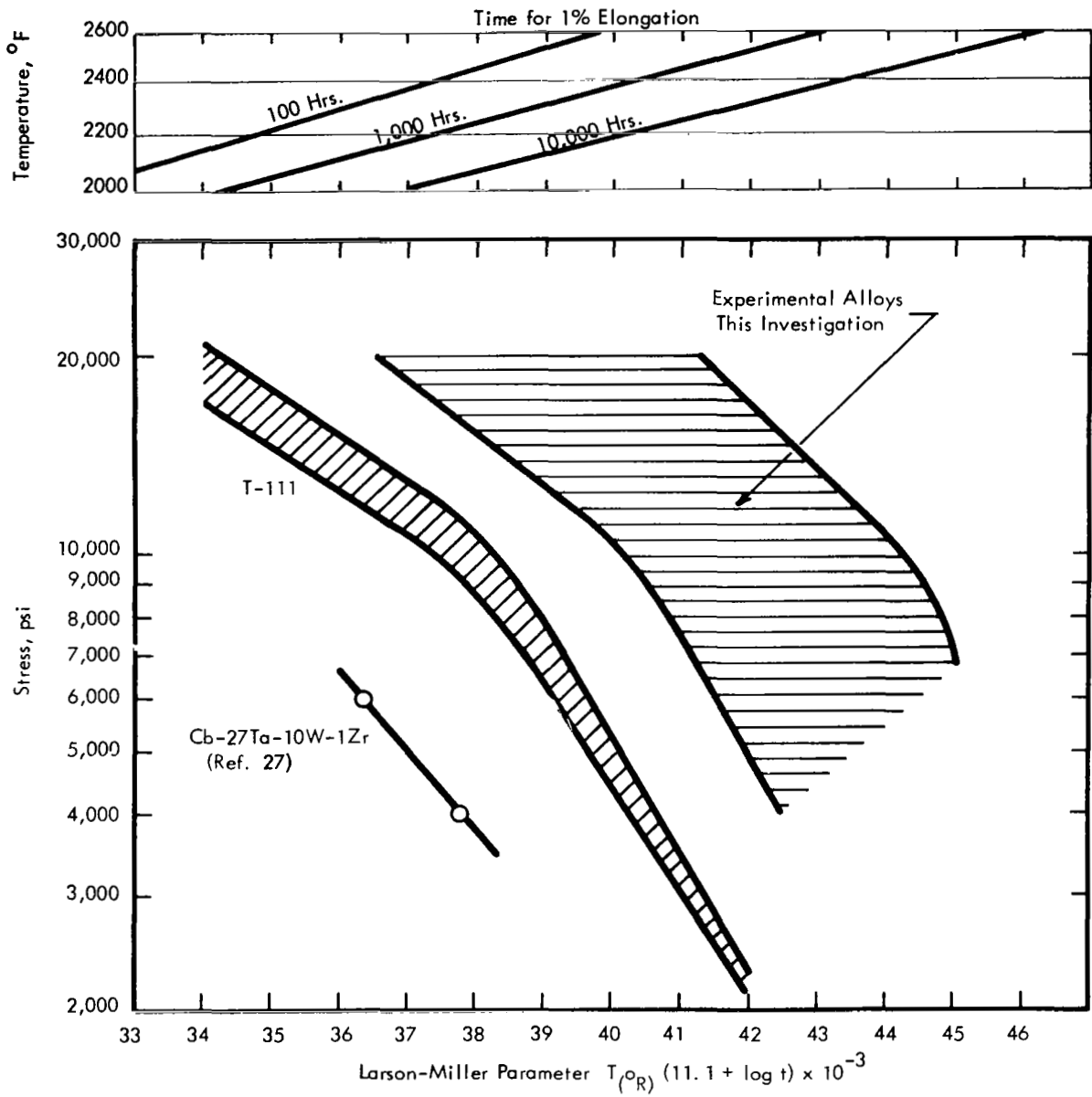
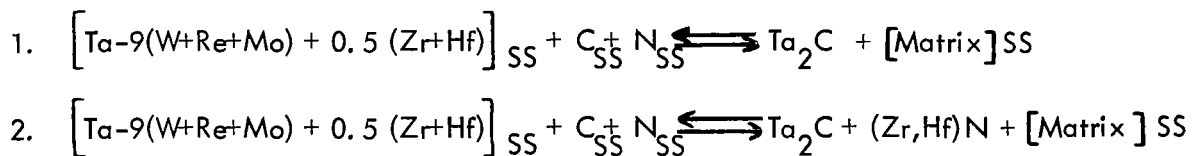


FIGURE 39 - Creep Behavior of Experimental Tantalum Base Alloys (t is Time in Hours to 1% Elongation)

7. Phase Relationships

The intersection of the four-phase fields in the tantalum-rich corner of the (Ta+W)-Hf-C phase diagram (2400°F) isotherm is shown in Figure 40. The composition of the precipitating carbide phase was not influenced by the tungsten content which ranged from 3-12% nor did the molybdenum or rhenium appear to effect the composition of the carbide. A tantalum-8-10W alloy containing 1%Hf would precipitate only the Ta₂C phase for all carbon concentrations up to 1000 ppm. The stabilization of the (HfTa)C_{1-x} did not occur until the reactive metal additions exceed 2% at the 100 ppm carbon level and about 3% at the 1000 ppm carbon level.

Substituting part of the carbon with nitrogen significantly altered the composition of the precipitating phases. Ta-W-Re-Mo alloys containing up to 0.5 atom percent Zr+Hf and up to 300 ppm carbon + nitrogen with the C/N atom ratio equal to unity precipitated two phases at 2400°F by the following reaction.



Reaction (1) occurred in solution annealed material subsequently aged for 1-16 hours at 2400°F.

Reaction (2) occurred on longer time aging i. e. , >>16 hours.

Increasing the reactive metal Zr+Hf above 3/4 atom percent resulted again in reaction 1 for short time aging exposure at 2400°F but on longer time aging, the Ta₂C phase completely disappeared and was replaced by the precipitation of a FCC phase identified as a (Hf,Ta)(C,N)_{1-x}. Although morphology of the Ta₂C phase can be significantly altered by heat treatment as discussed earlier, the composition remains unchanged.

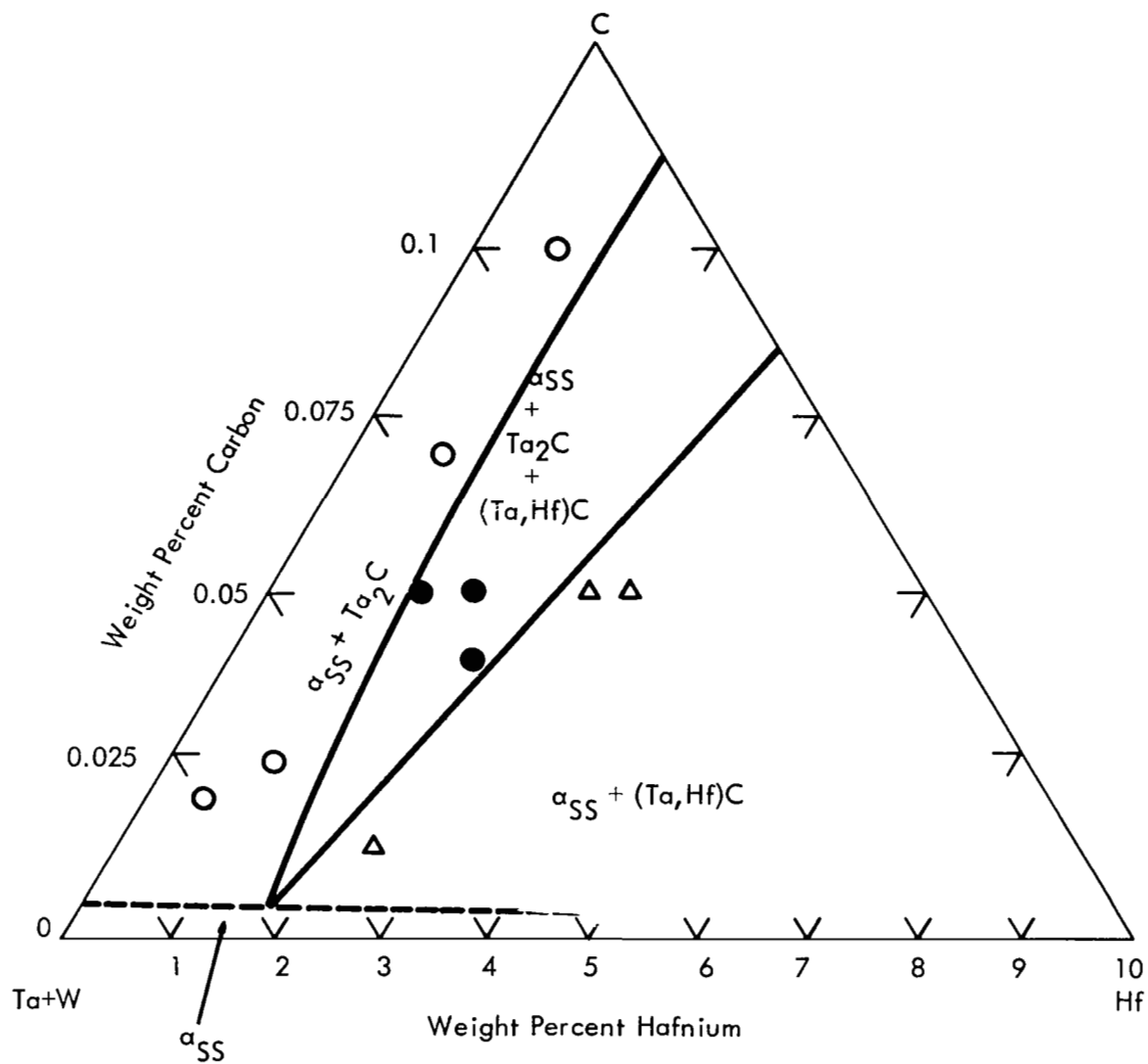


FIGURE 40 - Tantalum Rich Corner of the (Ta+W)-Hf-C Psuedo Ternary Phase Diagram (1315°C/2400°F) Isotherm

V. CONCLUSIONS

This was the first refractory metal alloy development program where primary emphasis was on optimizing long time creep properties. A significant advance has been made in tantalum technology with the development of ASTAR-811C, Ta-8W-1Re-0.7Hf-0.025C, a carbide dispersion strengthened tantalum alloy which has significantly better creep resistance than any commercially available tantalum alloy, and yet good fabricating and welding characteristics were retained.

A number of important conclusions which can be made from the results of this investigation are:

1. Carbides and nitrides are both effective creep strengtheners of tantalum alloy matrices.
2. From weldability and fabricability limitations, the carbon content should not exceed 300 ppm and from creep strength considerations should not be less than 200 ppm in an alloy containing 8-10% W+Re+Hf.
3. The (Ta+W)-Hf-C phase relationships have been defined and show that the Ta_2C is an effective dispersed phase for improving long time creep properties.
4. The amount of rhenium and hafnium are both critical. Optimum creep resistance is achieved with rhenium present in the amount of 0.5 to 1.5% and hafnium 0.5 to 1%.
5. The creep behavior can be significantly altered by changing the morphology of the Ta_2C precipitate by controlling final annealing practice.
6. Nitrides are more effective strengtheners than carbides below 2400°F since it has been shown that the reactive metal nitride precipitate has coherency with the tantalum alloy matrix.

Although significant advances have been made in tantalum alloy technology and significant improvements in creep strength have been achieved, much work yet remains to be done in identifying the role of the dispersed carbide or nitride phase in improving properties. Since fabricability and weldability limits the total substitutional solute additions, additional investigation of the role of thermal treatment and the effect of varying thermo-mechanical history is also warranted.

REFERENCES

1. R. W. Buckman, Jr. and R. C. Goodspeed, "Precipitation Strengthened Tantalum Base Alloys," Final Technical Report, WANL-PR-Q-017 Westinghouse Astronuclear Laboratory, Pittsburgh, Pa. (NASA CR-1642, 1970).
2. R. W. Buckman, Jr., "Effect of Environment on the Mechanical Properties of Refractory Metal Alloys", 1967 AVS Conference - June 11-13, 1967, New York, N. Y.
3. R. W. Buckman, Jr. and J. A. Hetherington, "An Apparatus for Determining Creep Behavior Under Conditions of Ultra-High Vacuum", Review of Scientific Instruments, Vol. 37, No. 8, August 1966.
4. J. C. Sawyer and E. A. Steigerwald, "Generation of Longtime Creep Data in Refractory Alloys at Elevated Temperature" - Final Report No. ER-7203, TRW, Inc., Cleveland, Ohio, June 4, 1967.
5. F. Garafalo, "Fundamentals of Creep and Creep Rupture in Metals", MacMillan Series in Materials Science.
6. A. L. Field, Jr., et al, "Research and Development of Tantalum and Tungsten Base Alloys", Final Report, Bureau of Naval Weapons, Contract NOw 50-852-C, May 26, 1961.
7. F. F. Schmidt, et al, "Investigation of Tantalum and Its Alloys", ASD-TDR 62-594, October, 1962.
8. F. F. Schmidt, et al, "Investigation of Tantalum and Its Alloys", ASD-TDR 62-594, Part II.
9. R. L. Ammon and R. T. Begley, "Pilot Production and Evaluation of Tantalum Alloy Sheet", Summary Phase Report, Contract NOw-62-0656-d, June 15, 1963 (WANL-RR-M-004).
10. R. L. Ammon and R. T. Begley, "Pilot Production and Evaluation of Tantalum Alloy Sheet", Summary Phase Report, Part II, Contract N600(19)-59762, July 1, 1964, (WANL-PR-M-009).
11. W. H. Chang, "A Study of the Influence of Heat Treatment on Microstructure and Properties of Refractory Alloys", ASD-TDR-62-211, February, 1962.
12. R. T. Begley et al, "Development of Columbium Base Alloy", WADC-TR-57-344, Part VII, April, 1963.

13. G. S. Ansell, "Mechanical Properties of Two-Phase Materials", International Symposium on High Temperature Technology, Asilomar Conference Grounds, California, September 8-11, 1963.
14. J. Weertman, *J. Appl. Physics*, Vol. 28, p. 362, 1957.
15. Anon., "Space Power Systems Advanced Technology Conference", Lewis Research Center, August 23-24, 1966, NASA-SP-131, pp 169-197.
16. J.R. DiStefano and E. E. Hoffman, "Corrosion Mechanism in Refractory Metal-Alkali Metal Systems", The Science and Technology of Tungsten, Tantalum, Molybdenum, Niobium and Other Alloys, Based on AGARD Conference, Oslo University Center, Oslo-Blindern, Norway, 23-26 June 1963, Pergamon Press, 1964, pp 275-285.
17. D. R. Stoner and G. G. Lessmann, "Measurement and Control of Weld Chamber Atmosphere", *Welding Journal Research Supplement*, August, 1965.
18. M. L. Pochon, et al, "The Solubility and Structure of Carbide Phases in Tantalum and Columbium", Vol. 2-Reactive Metals, Interscience Publications, pp 327-347.
19. H. R. Ogden, et al, "The Solubility of Carbon in Tantalum", *Trans. AIME*, Vol. 227, p. 1458-1460, December, 1963.
20. E. R. Storms, "A Critical Review of Refractories", Part I, Selected Properties of Group 4a, 5a and 6a Carbides, LAMS-2674, March, 1962.
21. H. D. Seghezzi, "New Investigations of the Tantalum Nitrogen System", 3rd Plansee Seminar, Reute, Austria, 1958.
22. L. Siegle, "Solid Solution Strengthening of Refractory Metals", AGARD Conference on Refractory Metals, Oslo University Centre, Oslo-Blindern, Norway, June 23-26, 1963.
23. F. F. Schmidt, et al, "Investigation of the Properties of Tantalum and Its Alloys", WADC-TR 59-13 (December 31, 1959).
24. R. T. Begley, et al, "Precipitation Hardening Columbium-Hafnium-Nitrogen Alloys", 5th Plansee Seminar, June 22-26, 1964, Reutte, Austria.
25. A. Kelley and R. B. Nicholson, "Precipitation Hardening", pp. 286-287, *Progress in Materials Science*, Vol. 10, No. 3, 1963.

26. R. H. Titran and R. W. Hall, "High Temperature Creep Behavior of a Columbium Alloy, FS-85", NASA-TND-2885, June, 1965.
27. R. H. Titran and R. W. Hall, "Ultra High Vacuum Creep Behavior of Columbium and Tantalum Alloys at 2000°F and 2200°F for Times Greater than 1000 Hours", NASA TND-3222, Jan. , 1966.
28. J. W. Clark, "Recent Developments in Columbium Base Alloys," Brochure from General Electric Co., February 19, 1965.